

A GAN-Based Data Poisoning Attack Against Federated Learning Systems and Its Countermeasure

Wei Sun, Bo Gao, *Member, IEEE*, Ke Xiong, *Member, IEEE*, Yuwei Wang
Pingyi Fan, *Senior Member, IEEE*, Khaled Ben Letaief, *Fellow, IEEE*

Abstract—As a distributed machine learning paradigm, federated learning (FL) is collaboratively carried out on privately owned datasets but without direct data access. Although the original intention is to allay data privacy concerns, "available but not visible" data in FL potentially brings new security threats, particularly poisoning attacks that target such "not visible" local data. Initial attempts have been made to conduct data poisoning attacks against FL systems, but cannot be fully successful due to their high chance of causing statistical anomalies. To unleash the potential for truly "invisible" attacks and build a more deterrent threat model, in this paper, a new data poisoning attack model named VagueGAN is proposed, which can generate seemingly legitimate but noisy poisoned data by untraditionally taking advantage of generative adversarial network (GAN) variants. Capable of manipulating the quality of poisoned data on demand, VagueGAN enables to trade-off attack effectiveness and stealthiness. Furthermore, a cost-effective countermeasure named Model Consistency-Based Defense (MCD) is proposed to identify GAN-poisoned data or models after finding out the consistency of GAN outputs. Extensive experiments on multiple datasets indicate that our attack method is generally much more stealthy as well as more effective in degrading FL performance with low complexity. Our defense method is also shown to be more competent in identifying GAN-poisoned data or models. The source codes are publicly available at <https://github.com/SSsWEIssSS/VagueGAN-Data-Poisoning-Attack-and-Its-Countermeasure>.

Index Terms—Federated learning, Security and Privacy, Generative Adversarial Networks, Data Poisoning

I. INTRODUCTION

Emerging as a promising distributed learning paradigm, federated learning (FL) can be used to collaboratively train a deep learning model at a server based on decentralized datasets privately owned by multiple clients. Compared with traditional distributed learning approaches, FL has several

advantages: a) massive amounts of previously inaccessible on-device data and computing power resources can be utilized; b) clients' private datasets are not shared and uploaded so that data privacy can be protected and communication bandwidth can be saved; c) potentially unlimited on-device resources can be crowdsourced. Therefore, FL will probably become a fundamental feature of most smart devices or their digital twins.

However, the "available but not visible" nature of training data in FL leads to security risks. A server usually has to rely on the support of a large number of possibly untrustworthy clients, because it is very likely that some of the clients especially crowdsourced ones are originally manipulated or hijacked by some attackers. More seriously, the server does not have access to the clients' private datasets that largely determine the quality of training outcomes, so the local data "not visible" to the server or the resulting local models can easily become the best targets of the attackers.

Poisoning attacks are the greatest threats in an FL system. An insider attacker can falsify either the local data (via data poisoning) or the local models (via model poisoning) of compromised clients to indirectly mislead the global model of a server that is built upon those local data or models. Theoretically, such poisoning attacks can be not only effective in undermining the global model but also undetectable by the server without data access. In comparison with the model poisoning attacks, the data poisoning attacks are generally harder to be detected by the server and thus would be more worth studying [2].

It is still very challenging to carry out both effective and stealthy data poisoning attacks against FL systems, though some initial attempts have been made [2]–[7]. Existing attack methods primarily leverage e.g. label flipping techniques to generate poisoned local data through falsifying the labels of training data [8]–[11]. These attack methods can globally degrade FL outcomes, but they inevitably give rise to significant changes in local label distributions that can be readily detected by existing defense methods based on statistical analysis [8], [12]–[15]. As a result, the data poisoning attacks at this stage are not truly threatening. However, they still show great potential in producing seemingly legitimate poisoned data without unusual statistical characteristics, so we must get fully prepared.

In this paper, we propose to poison local data for FL using certain variants of generative adversarial network (GAN) [16] to ensure effective, efficient, and stealthy attacks. Instead of producing near-realistic data of high quality through regular

The preliminary results of this paper have been presented in part in IEEE SECON 2023. This work was supported in part by the Fundamental Research Funds for the Central Universities under Grant 2021JBM008 and Grant 2022JBXT001, and in part by the National Natural Science Foundation of China (NSFC) under Grant 61872028. (Corresponding author: Bo Gao.)

W. Sun, B. Gao and K. Xiong are with the Engineering Research Center of Network Management Technology for High Speed Railway of Ministry of Education, School of Computer Science and Technology, and the Collaborative Innovation Center of Railway Traffic Safety, Beijing Jiaotong University, Beijing 100044, China. E-mail: {21120398, bogao, kxiong}@bjtu.edu.cn.

Y. Wang is with the Institute of Computing Technology, Chinese Academy of Sciences, Beijing 100190, China. E-mail: wangyuwei@ict.ac.cn.

P. Fan is with the Beijing National Research Center for Information Science and Technology, and the Department of Electronic Engineering, Tsinghua University, Beijing 100084, China. E-mail: fpy@tsinghua.edu.cn.

K. Letaief is with the Department of Electrical and Computer Engineering, Hong Kong University of Science and Technology, Hong Kong 999077, China. E-mail: eekhaled@ust.hk.

uses of GAN, our attack method turns to reversely leverage the power of GAN to generate vague data with appropriate amounts of poisonous noise. The local models poisoned by such vague data can be made globally damaging, while the vague data can mostly keep the statistical characteristics of their GAN inputs so that the local models poisoned can be seemingly legitimate. In addition, it can be computationally efficient to generate vague data of relatively low quality, rendering it broadly applicable, even for resource-constrained mobile devices. To thwart such attacks, we further propose to capture the characteristics of GAN outputs so as to identify GAN-poisoned data or models. In order to address the security threats in FL more effectively and establish a safer and more robust FL system, our contributions are as follows.

- We propose an attack method named *VagueGAN*, which is a GAN model specially designed for data poisoning attacks against FL systems. It generates vague poisoned data that can not only effectively but also unnoticeably attack a global model with all labels/classes involved. To the best of our knowledge, it is the first GAN model with emphasis on direct generation of FL-targeted poisoned data for improved attack stealthiness.
- We develop guidelines for taking full advantage of *VagueGAN* to achieve a balanced trade-off between attack effectiveness and stealthiness, which is not readily achievable for existing approaches.
- We further propose an unsupervised variant of *VagueGAN* for broader applicability, which generates poisoned data without relying on the labels of training data and without compromising its effectiveness and stealthiness.
- We propose a cost-effective countermeasure named *Model Consistency-Based Defense (MCD)* to this type of data poisoning attacks, which directly reuses the local models already collected by the server to identify GAN-poisoned data or models based on our findings on the consistency of GAN outputs.
- We conduct extensive experiments on multiple most-used datasets: CIFAR-10, MNIST and Fashion-MNIST. It is verified that data poisoning attacks enhanced by our *VagueGAN* not only better degrade FL outcomes with low efforts but also are generally much less detectable. Our defense method is also shown to be effective in identifying GAN-poisoned data or models.

The remainder of this paper is organized as follows. Related work is discussed in section II. Objectives and assumptions are outlined in section III, where the system model and attack model are defined. Our proposed *VagueGAN* model and data poisoning attacks based on it are elaborated in section IV. Our proposed defense method is suggested in section V. Performance evaluation is presented in section VI. Finally, our conclusions and future work are summarized in section VII.

II. RELATED WORK

Although data poisoning attacks against regular deep learning systems have been well studied [17]–[21], the research on those against FL systems is still in its infancy. Existing work primarily leverages label flipping techniques to generate

poisoned local data through falsifying certain labels of training data. Specifically, article [8] proposes a label flipping attack to rearrange the label-sample associations of a local dataset to generate a poisoned dataset. In addition, article [17] proposes a GAN model for the first time to extract private features of local data from GAN-generated pseudo data after initializing the GAN by the global model. On this basis, article [9] proposes to enhance regular label flipping attacks by their *PoisonGAN*, an off-the-shelf GAN model only used to enlarge the sizes of local datasets with legitimate pseudo samples by using a discriminator initialized by the global model. Article [22] proposes to invert a benign model’s loss function to create malicious gradients, which are then used to poison the labels of local data samples. Article [23] proposes a clean-label poisoning attack by adding a perturbation to the gradients of adversarial loss, which only generates poisoned features, without falsifying labels. However, these attack methods inevitably give rise to significant changes in the local distributions of training data, which can be readily detected by corresponding defense methods.

To mitigate data poisoning attacks against FL systems, some countermeasures have been found to be useful. On the one hand, some existing works [8], [12], [14], [24]–[27] employ similar two-step statistical approaches, where lower-dimensional local models are obtained in the first step and are directly analyzed for outlier detection in the second step. Specifically, article [8] and [12] propose principal component analysis (PCA) and uniform manifold approximation and projection (UMAP) respectively to reduce the dimensions of all local models to two-dimensional, to facilitate the identification of any abnormal model distribution. Article [24] proposes divide-and-conquer (DnC), which computes the distance between the maximum variance direction of all local models and the updated scalar product. Article [25] proposes *FLDetector*, where the server predicts every client’s model updates and flags a client as malicious there is a multi-round mismatch between the client’s actually uploaded model updates and its predicted ones. Article [26] proposes a label-flipping-robust (LFR) algorithm based on cosine similarity temporal analysis, which is applicable to both independent and identically distributed (IID) and non-IID data. Article [27] proposes *CONTRA*, which implements a cosine-similarity-based measure. Article [14] proposes local malicious factor (*LoMar*), which is based on the kernel density estimation and k-nearest neighbor methods.

On the other hand, some defense methods [28]–[34] detect malicious clients by leveraging additional resources or tools to characterize and identify abnormal local models or datasets. Specifically, article [28] proposes to utilize a global test dataset to identify abnormal local models. Article [29] proposes ensemble federated learning, which trains multiple global models and utilizes a test dataset to validate their security levels. Article [30] uses GANs to generate auditing data in the training procedure and removes adversaries by auditing their model accuracy. Article [31] proposes a framework with encoder-decoder architecture, which identifies malicious local models in low-dimensional latent feature space. Article [32] proposes a generator to learn the knowledge of global model

over the latent feature space, and such a feature extraction can help identify malicious clients whose local data is found to be of low quality. Article [33] requires each client to individually identify poisoned labels of its local data using the global model given by the server and learn from the poisoned data using a generator. Article [34] proposes DPA-FL, a method that tests local models with a separate global dataset and identifies outliers with low model accuracy. However, none of these defense methods works well if attackers can generate seemingly legitimate poisoned data whose statistical distributions approximate normal ones.

III. OBJECTIVES AND ASSUMPTIONS

In this section, we describe the objectives and assumptions regarding data poisoning attacks against an FL system.

A. System Model

We consider an FL system that consists of a server and a set $\mathcal{C} = \{c_1, c_2, \dots, c_N\}$ of N mobile clients. A regular training process of FL is considered. Initially, the server distributes an FL main task to each client. In each round $t = 1, 2, \dots, T$ of FL, every client c_i receives model updates from the server and trains a local model $\theta_{t,i}$ on its local dataset \mathcal{D}_i^{train} . To avoid potential network congestions, the server then randomly selects K out of N clients, aggregates their local models into a global model $\tilde{\theta}_t$ and sends it to all the clients for a new round of training. Meanwhile, the server uses a test dataset \mathcal{D}^{test} to obtain the global accuracy a_t of $\tilde{\theta}_t$.

B. Attack Model

a) Attacker's goal: In an FL system, we assume that there exists at least one data poisoning attacker. The attacker's primary goal is to degrade the performance of the global model as much as possible. Second, the attacker's another equally important goal is to hide its attacks from being detected by the server.

b) Attacker's capabilities: The attacker is assumed to be capable of carrying out data poisoning attacks. First, the attacker can gain control of one or more benign clients or disguise itself as a benign client. Second, the attacker can gain all the privileges of each controlled client, e.g., local dataset, local model training process, etc.

Due to our focus on data poisoning attacks, the attacker's scope of operation is assumed to be limited to every controlled client. First, we guarantee that the server is completely honest and unattackable. Second, we assume that communication links for FL are reliable and the attacker cannot influence the process of model exchanges over the links. Third, the attacker cannot access any datasets of the server and uncontrolled clients. Finally, the attacker also has no access to the models of uncontrolled clients.

c) Attacker's approach: The attacker carries out a data poisoning attack to achieve its goals. In particular, the attacker first obtains control of at least one client as malicious client through certain means. Then the attacker poisons the local dataset of the malicious client and obtains a poisoned local

dataset using an attack method. Finally, the malicious client trains a poisoned local model on its poisoned local dataset and uploads it to the server. If not being detected by the server, the poisoned local model is expected to harm the global model after model aggregation.

IV. GAN-BASED DATA POISONING ATTACKS

In this section, we propose a new GAN model called "VagueGAN", which is specifically designed for data poisoning attacks against FL systems.

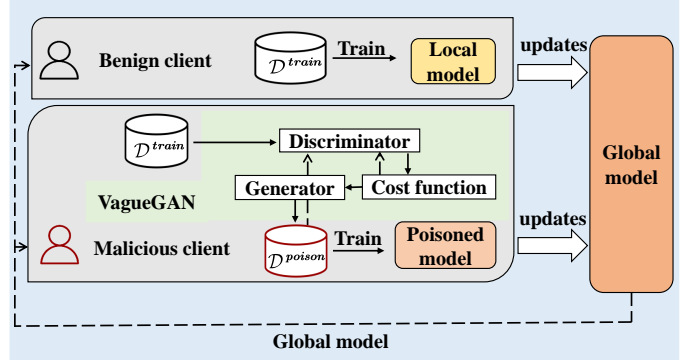


Fig. 1: Use of VagueGAN for a data poisoning attack

A. VagueGAN Poisoning Attack

Following the regular attack approach, the attacker can easily conduct a data poisoning attack based on our VagueGAN, as shown in Figure 1. Specifically, the attacker first obtains the control of client c_j . Then malicious client c_j uses VagueGAN to generate a poisoned local dataset \mathcal{D}_j^{poison} and replaces the original dataset \mathcal{D}_j^{train} . Finally, client c_j uses \mathcal{D}_j^{poison} to train and upload a poisoned local model $\theta_{t,j}^{poison}$ to the server. Unlike a label flipping attack that only affects selected labels, our VagueGAN indirectly attacks a global model with all labels/classes involved.

B. VagueGAN Model

A GAN model has a generator G and a discriminator D . On the one hand, the generator G generates fake data samples close to real ones and tries to convince the discriminator D . On the other hand, the discriminator D tries to distinguish between real and fake samples. They compete with each other in the training phase, thus operating as an adversarial game that makes the generator G approximate original data distribution.

Our VagueGAN unconventionally leverages the power of GAN to generate seemingly legitimate vague data with appropriate amounts of poisonous noise, in order to achieve a balanced trade-off between attack effectiveness and stealthiness. On the one hand, VagueGAN needs to generate seemingly legitimate poisoned data for a stealthy attack. We extend the Conditional GAN (CGAN) model [35] to generate poisoned data from legitimate local data. The architectures of the generator and discriminator of VagueGAN have been optimised

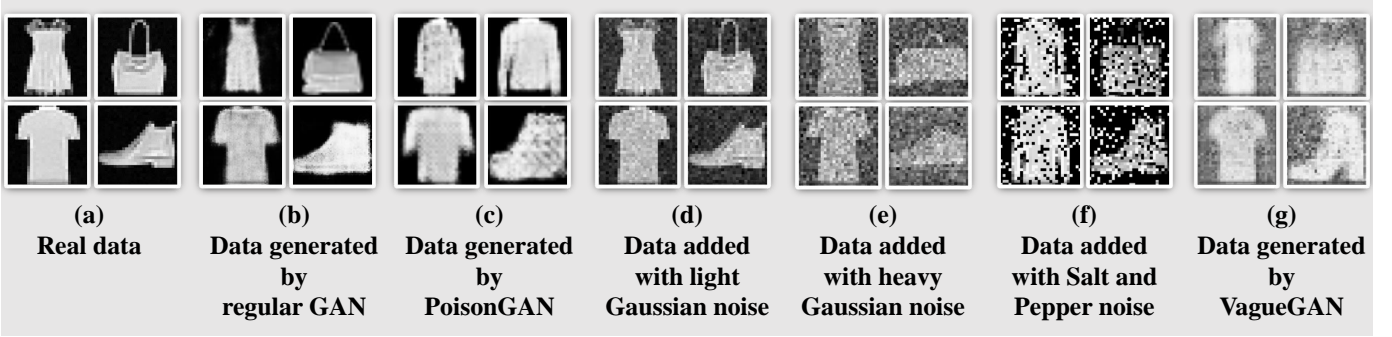


Fig. 2: Comparison of noise-superimposed samples and samples generated by different GANs

in order to achieve superior poisoning results. Similar to the original CGAN, all data is generated through a multi-layer perceptron (MLP)-like network. Beyond the original CGAN, however, three enhancements are put in place for VagueGAN to make resulting poisoned data closer to legitimate ones. First, VagueGAN utilizes a much deeper structure in the discriminator (4 hidden layers). A deeper discriminator improves attack stealthiness by ensuring that the poisoned data better retains legitimate features even from a small local dataset. Second, VagueGAN also employs techniques such as batch normalization and LeakyReLU to more effectively capture data features. Third, VagueGAN adopts a large batch size for full dataset training to further obtain the overall features of local dataset.

On the other hand, VagueGAN needs to generate noisy poisoned data for an effective attack, since data noise can easily harm the quality of training data and thus that of resulting trained model. First, besides the discriminator, VagueGAN also utilizes a much deeper structure in the generator (4 hidden layers) and techniques such as batch normalization and LeakyReLU. A deeper generator improves attack effectiveness by increasing the uncertainty of data generation and thus making the poisoned data vaguer and noisier. Second, we design a loss function of VagueGAN to break the commonly reached Nash equilibrium between the generator and the discriminator by restricting the discriminative ability of the discriminator. This can lower the generation performance of the generator and thus lead to generated data carrying a lot of poisonous noise.

Our loss function is defined as follows:

$$\min_G \max_D V(G, D) = \mathbb{E}_{\mathbf{x} \sim p_d(\mathbf{x})} [\log(1 + \kappa)D(\mathbf{x})] + \mathbb{E}_{\mathbf{z} \sim p_z(\mathbf{z})} [\log(1 - (1 + \kappa)D(G(\mathbf{z})))] \quad (1)$$

where \mathbf{x} is a sample following the original data distribution $p_d(\mathbf{x})$; \mathbf{z} is the sample obtained from a certain distribution $p_z(\mathbf{z})$; $G(\mathbf{z})$ is the fake sample generated by the generator G ; $D(\mathbf{x})$ represents the probability that \mathbf{x} is a real sample. On the one hand, the larger $D(\mathbf{x})$ (or $D(G(\mathbf{z}))$) is, the more accurately the discriminator D can identify original (or generated) samples. Hence, stronger D is obtained to maximize V . On the other hand, if G is stronger, the discriminator will make a misjudgment, and $D(G(\mathbf{z}))$ will become larger. Hence, stronger G is obtained to minimize V . We use a suppression

factor $\kappa \in (0, 1)$ to limit the generation ability of the generator G . The larger value of κ is, the more restrictive it is on the generation ability. Clearly, the value of κ can be used to deal with the trade-off between the effectiveness and stealthiness of VagueGAN. The steps for conducting a VagueGAN poisoning attack are summarized in Algorithm 1.

The training process of VagueGAN is similar to those of traditional GANs [35], where the generator and discriminator undergo iterative optimization through an adversarial game.

To support data poisoning attacks, on the one hand, the generation target of our VagueGAN is much different from that of traditional GANs for regular uses. As shown in Figure 2(b) and 2(g) taking image data as an example, the sample distribution generated by a traditional GAN is largely fitted to the real sample distribution, but that generated by VagueGAN is just roughly close to the real sample distribution for a balanced trade-off between seemingly legitimate and noisy results. The samples generated by PoisonGAN (Figure 2(c)) with discriminator D initialized by the global model [9] are also of relatively good quality because PoisonGAN can be considered as a data augmentation method instead of an actual attack method. Furthermore, compared with traditional GANs, our VagueGAN can be more computationally efficient only aiming to generate vague data of relatively low quality. Note that even if being under-trained for data poisoning, traditional GANs usually generate intermediate outputs with certain vagueness but without carrying noise, and thus cannot ensure successful attacks.

On the other hand, the vague data generated by VagueGAN is different from real data superimposed with noise (Figure 2(d), 2(e) and 2(f)). Adding noise directly to real data produces poisoned data whose attack quality is very difficult to control. Intuitively, better attack effectiveness can be achieved by making a noise level higher, but this can make the noise more noticeable and thus leading to worse attack stealthiness. This is because the manually added noise (e.g. Gaussian, Salt and Pepper (SAP) [36]) has nothing related to the original data statistically. In contrast, the noise generation of VagueGAN is guided by the statistics of original data, so that the GAN-generated noise can more smoothly fit the original data than the manually added noise. Our experiments will show that only our VagueGAN can flexibly control the quality of vague data on demand to strike a balance between attack effectiveness and stealthiness.

Algorithm 1 VagueGAN poisoning attack algorithm

Input: Client c_j 's local training dataset \mathcal{D}_j^{train}
Output: Poisoned local training dataset \mathcal{D}_j^{poison} ; local model parameters $\theta_{t,j}^{poison}$

- 1: **Initialization:** Number of training epochs E for VagueGAN; generator suppression factor κ ; number of training rounds T for FL
- 2: Deploy the VagueGAN model at a controlled client c_j and receive an FL training task from the server.
- 3: //Poisoned Data Generation
- 4: **for** $e = 1, 2, \dots, E$ **do**
- 5: Set training batch = \mathcal{D}_j^{train}
- 6: Train the VagueGAN model on \mathcal{D}_j^{train} according to (1)
- 7: **end for**
- 8: Get outputted \mathcal{D}_j^{poison}
- 9: //FL Training Task
- 10: **for** $t = 1, 2, \dots, T$ **do**
- 11: Receive the global model $\tilde{\theta}_t$ from the server
- 12: Train the local model $\theta_{t,j}$ on $\tilde{\theta}_t$ and \mathcal{D}_j^{poison}
- 13: Get outputted $\theta_{t+1,j}^{poison}$ and upload it to the server
- 14: **end for**

C. Theoretical Analysis

This subsection aims to theoretically reveal the characteristics of poisoned data generated by VagueGAN. For the expectation form of the loss function in Equation (1), we rewrite it in integral notation as follows:

$$\min_G \max_D V(G, D) = \int_{\mathbf{x}} p_d(\mathbf{x}) \log(1 + \kappa)D(\mathbf{x})d\mathbf{x} + \int_{\mathbf{z}} p_z(\mathbf{z}) \log(1 - (1 + \kappa)D(G(\mathbf{z})))d\mathbf{z} \quad (2)$$

The data distribution learned by the generator G is represented as $p_g(\mathbf{x})$. According to the Law of the Unconscious Statistician (LOTUS) theorem [37], by replacing \mathbf{z} using its mapping to \mathbf{x} and then transforming it into an integral form, we can obtain an alternative expression for (4):

$$\min_G \max_D V(G, D) = \int_{\mathbf{x}} [p_d(\mathbf{x}) \log(1 + \kappa)D(\mathbf{x}) + p_g(\mathbf{x}) \log(1 - (1 + \kappa)D(\mathbf{x}))]d\mathbf{x} \quad (3)$$

For a fixed generator G , our objective is to solve for $\max_D V(G, D)$, which entails finding the optimal discriminator D^* that maximizes the right-hand side of the equation.

$$\max_D V(G, D) = \int_{\mathbf{x}} [p_d(\mathbf{x}) \log(1 + \kappa)D(\mathbf{x}) + p_g(\mathbf{x}) \log(1 - (1 + \kappa)D(\mathbf{x}))]d\mathbf{x} \quad (4)$$

In Equation (4), $p_d(\mathbf{x})$ refers to the probability of sampling a sample \mathbf{x} from the distribution p_d , $p_g(\mathbf{x})$ refers to the probability of sampling a sample from the generator G , and $D(\mathbf{x})$ represents a mapping of $x \in \mathbb{R}$. The maximization of the integral in Equation (4) can be reformulated as finding

the maximum value of the integrand, through determining the optimal discriminator D . Consequently, during this process, the probabilities associated with the real data distribution $p_d(\mathbf{x})$ and the generated data distribution $p_g(\mathbf{x})$ can be treated as constants. Taking the partial derivatives of both sides of the equation with respect to D , we obtain:

$$\begin{aligned} \frac{\partial}{\partial D} (\max_D V(G, D)) &= \int_{\mathbf{x}} \frac{\partial}{\partial D} [p_d(\mathbf{x}) \log((1 + \kappa)D(\mathbf{x})) \\ &\quad + p_g(\mathbf{x}) \log(1 - (1 + \kappa)D(\mathbf{x}))]d\mathbf{x} \quad (5) \\ &= \int_{\mathbf{x}} \left[p_d(\mathbf{x}) \frac{1}{D(\mathbf{x})} + p_g(\mathbf{x}) \frac{-(1 + \kappa)}{1 - (1 + \kappa)D(\mathbf{x})} \right] d\mathbf{x} \end{aligned}$$

By taking further derivatives of Equation (5), it can be determined that Equation (4) is a convex function. Therefore, Equation (4) attains a unique maximum value at the point where its first derivative is equal to zero. At this point, we have:

$$D^*(\mathbf{x}) = \frac{p_d(\mathbf{x})}{(1 + \kappa)(p_d(\mathbf{x}) + p_g(\mathbf{x}))} \quad (6)$$

When $D^*(\mathbf{x}) = 0.5$, the specially designed discriminator in VagueGAN is unable to distinguish between real samples and samples generated by the generator. At this point, the generator of VagueGAN reaches its generation bottleneck. Consequently, we can conclude that:

$$p_g(\mathbf{x}) = \frac{(1 - \kappa)}{(1 + \kappa)} p_d(\mathbf{x}) \quad (7)$$

Equation (7) reveals that VagueGAN has a distinct generation objective compared to traditional GANs. When VagueGAN achieves optimal performance, the distribution of the generated poisoned data is related to the original data distribution, but not identical. This distinction arises from the unique suppression factor κ in VagueGAN. By adjusting the suppression factor κ , VagueGAN can control the level of conformity between the generated poisoned data and the real data. Within the feasible range of κ ($\kappa \in (0, 1)$), a higher value of κ leads to a reduced correlation between the poisoned data and the real data, while a lower value of κ yields a higher correlation. When κ equals 0, VagueGAN is equivalent to a regular GAN.

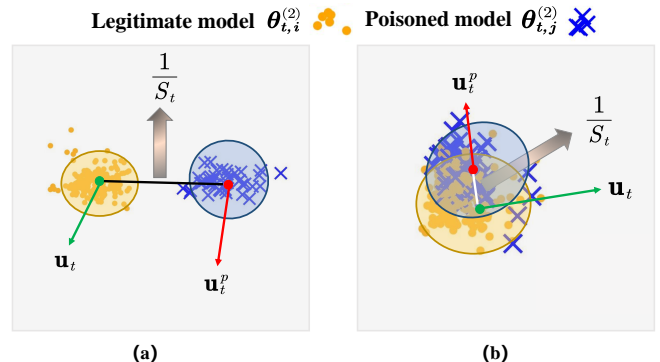


Fig. 3: Different levels of attack stealthiness

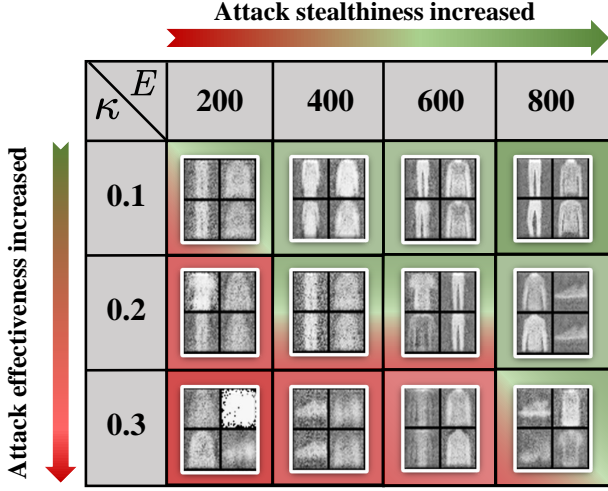


Fig. 4: Trade-off between attack effectiveness and stealthiness

D. Attack Effectiveness-Stealthiness Trade-off

There is usually a trade-off between attack effectiveness and stealthiness. Noisier data generated by VagueGAN can be more effective in degrading FL performance, but may bring greater data statistical changes and thus may be easier to detect. Therefore, the attacker needs to make appropriate settings for VagueGAN to fine-tune the quality of vague data and achieve a balanced trade-off between attack effectiveness and stealthiness. Here we give some guidelines for taking full advantage of VagueGAN for the balanced trade-off.

The effectiveness A_t of an attack in round t of FL can be characterized by the drop in the accuracy of global model from a_t to a_t^p due to the presence of the attack:

$$A_t = a_t - a_t^p \quad (8)$$

The stealthiness S_t of an attack in round t of FL can be characterized by the statistical distance between legitimate and poisoned models. Since local model $\theta_{t,i}$ is very high-dimensional, we first use PCA to downscale $\theta_{t,i}$ to 2-dimensional $\theta_{t,i}^{(2)}$.

$$\theta_{t,i}^{(2)} = \text{PCA}(\theta_{t,i}) \quad (9)$$

Then, we separate all legitimate local models and poisoned local models into two clusters and find the centroids \mathbf{u}_t and \mathbf{u}_t^p of these two clusters, respectively.

$$\mathbf{u}_t = \frac{\sum_{i=1}^{N-M} \theta_{t,i}^{(2)}}{N-M} \quad (10)$$

$$\mathbf{u}_t^p = \frac{\sum_{j=1}^M \theta_{t,j}^{(2)}}{M} \quad (11)$$

where N is the number of all clients and M is the number of malicious clients, so $N - M$ is the number of benign clients. We use the reciprocal of the Euclidean distance \mathbf{E} between \mathbf{u}_t and \mathbf{u}_t^p to measure S_t :

$$S_t = \frac{1}{\mathbf{E}(\mathbf{u}_t, \mathbf{u}_t^p)} = \frac{1}{\|\mathbf{u}_t - \mathbf{u}_t^p\|} \quad (12)$$

For example, Figure 3 shows two different cases with different levels of attack stealthiness S_t . The performance of S_t is lower (or higher) as in Figure 3(a) (or 3(b)) when the statistical distance between legitimate and poisoned models is larger (or smaller).

To study the trade-off between attack effectiveness A_t and stealthiness S_t , we have analyzed the experimental outputs of VagueGAN. Clearly, the trade-off is closely related to the quality of poisoned data generated by VagueGAN. The more VagueGAN learns the characteristics of legitimate data, the higher stealthiness but lower effectiveness the resulting attack can achieve, and vice versa. In follow-up experiments, it has been found that there are two important factors affecting the quality of poisoned data: VagueGAN training epochs E and generator suppression factor κ . A balanced trade-off between attack effectiveness A_t and stealthiness S_t can be achieved by setting the values of E and κ appropriately. E is set to make VagueGAN stay in a semi-fitting state, and κ is adjusted to limit the generation ability of the generator of VagueGAN. For example, poisoned data of balanced quality around the middle area in Figure 4 can be generated by experimentally setting $E \in [400, 600]$ and $\kappa = 0.2$. More details can be found in subsection VI-C.

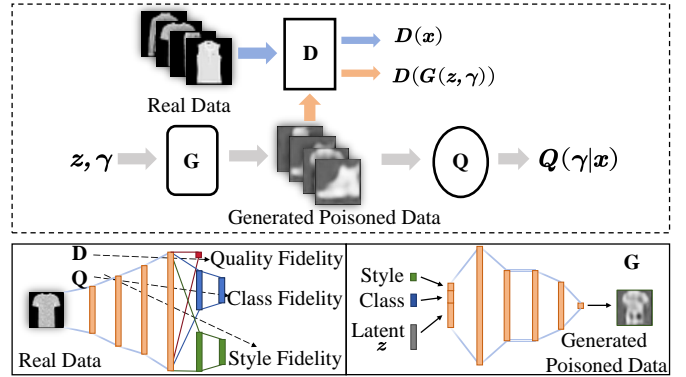


Fig. 5: The architecture of unsupervised VagueGAN

E. Unsupervised Variant of VagueGAN

Sometimes the attacker may not have full access to the label information of a local dataset, making the generation of poisoned data even more challenging. Inspired by InfoGAN [38], we further propose an unsupervised variant of VagueGAN for broader applicability. As shown in Figure 5, unsupervised VagueGAN could not only learn to generate realistic samples but also learn auxiliary features (class fidelity and style fidelity). Similar to supervised generation, unsupervised VagueGAN also replaces the original distribution of data with a conditional distribution. The main difference lies in that unsupervised VagueGAN does not require feeding label and attribute information into the discriminator network. Instead, it utilizes another classifier Q to learn auxiliary features.

As shown in Figure 5, both the discriminator and generator networks of unsupervised VagueGAN consist of 4 hidden layers. Unsupervised VagueGAN uses an additional classifier network Q to measure the validity of the auxiliary vector. This additional classifier shares most of its weights (the first 4 hidden layers) with the discriminator.

The objective function of unsupervised VagueGAN is defined as follows, with an addition $-\lambda L(G, Q)$, to Equation (1):

$$\begin{aligned} \min_{G, Q} \max_D V(G, D, Q) = & \mathbb{E}_{x \sim p_d(x)} [\log(1 + \kappa)D(x)] + \\ & \mathbb{E}_{z \sim p_z(z), \gamma \sim p(\gamma)} [\log(1 - (1 + \kappa)D(G(z, \gamma)))] \\ & - \lambda L(G, Q) \end{aligned} \quad (13)$$

where λ is hyperparameter, $x \sim G(z, \gamma)$ is the generated poisoned data, and γ represents auxiliary information, which includes class fidelity and style fidelity generated from classifier Q . $p(\gamma)$ describes the actual distribution of γ , which is rather hard to obtain. Therefore, VagueGAN uses the posterior distribution, $Q(\gamma|x)$, to estimate $p(\gamma)$, and this process is done with a neural network classifier. $L(G, Q)$ is an approximation of mutual information (lower bound of mutual information [38]), $I(\gamma; G(z, \gamma))$, between the auxiliary vector and generated poisoned sample:

$$\begin{aligned} L(G, Q) = & \mathbb{E}_{\gamma \sim p(\gamma), x \sim G(z, \gamma)} [\log Q(\gamma|x)] + H(\gamma) \\ = & \mathbb{E}_{x \sim p_G(x|z, \gamma)} E_{\gamma \sim p(\gamma|x)} \log Q(\gamma|x) + H(\gamma) \\ \leq & I(\gamma; G(z, \gamma)) \end{aligned} \quad (14)$$

Mutual information, $I(\gamma; G(z, \gamma))$, describes how much VagueGAN knows about random variable γ based on knowledge of $G(z, \gamma)$, i.e. $I(\gamma; G(z, \gamma)) = H(\gamma) - H(\gamma|G(z, \gamma))$, in which $H(\gamma)$ is conditional entropy. It can also be described by the Kullback-Leibler divergence, the information loss when using marginal distributions to approximate the joint distribution of γ and $G(z, \gamma)$.

Thanks to the unique loss function, the effectiveness and stealthiness of supervised and unsupervised VagueGAN attacks are comparable. Detailed evaluation results can be found in subsection VI-D.

F. Deployment Considerations

VagueGAN can be readily deployable in practice. First, VagueGAN is relatively easy to train. VagueGAN introduces a unique loss function that prevents from generating high-quality data unnecessary for attack purpose. In addition, VagueGAN does not have to wait for the convergence to a Nash equilibrium to obtain relatively low-quality but damaging poisoned data, leading to substantially reduced training efforts and costs compared to regular GANs. The adoption of full dataset training also demands fewer epochs to generate expected poisoned data. The limitations inherent to a regular GAN, such as non-convergence and unstable training, do not hinder the use of VagueGAN. In comparison, the original GAN is unable to generate data that meets the requirements for poisoning attacks. Even its intermediate outputs during the generation process

can only achieve a degree of "vagueness" without carrying "noise". Additionally, even with simpler models, achieving its generation goal is associated with high training costs. Second, VagueGAN only incurs one-time cost. It requires to build up a loss function from available datasets only once, enabling the generation of an arbitrary amount of poisoned data thereafter. Third, VagueGAN can be flexibly deployed depending on the attacker's resource availability. In general, there are three ways to put VagueGAN into use, including distributed deployment, centralized deployment, and hybrid deployment, so it is not hard for the attacker to find a way to deploy VagueGAN.

Distributed Deployment: As shown in Figure 6(a), if the attacker has gained the control of one or more clients with rich on-device resources, a VagueGAN model can be individually trained on each of the malicious clients, giving diversified poisoned datasets. When we use the term "VagueGAN" in this paper, we will mean VagueGAN implementing a distributed deployment, unless we state otherwise.

Centralized Deployment: As shown in Figure 6(b), if the attacker has access to a resource-rich platform reachable from the clients, one or more VagueGAN models can be centrally trained after collecting local data from the malicious clients. Then either unified or diversified poisoned datasets can be distributed to the malicious clients.

Hybrid Deployment: As shown in Figure 6(c), if some of the malicious clients have rich on-device resources but others do not, a mixture of locally trained and centrally trained VagueGAN models can be applied.

V. MODEL CONSISTENCY-BASED DEFENSE

Thanks to its inherent generative capability, our VagueGAN can generate seemingly legitimate poisoned data and thus can bypass existing defense methods. In this section, we analyze the characteristics of GAN outputs and suggest a model consistency-based countermeasure to GAN-based data poisoning attacks. Our defense method is effective when the same VagueGAN model is consistently applied by the attacker, though the idea of VagueGAN still has great potential to deliver undetectable attacks if implemented in varying settings. Moreover, our defense method also works against mainstream data poisoning attacks.

A. Local Model Analysis

To find a clue for the identification of malicious clients given that the server does not have access to any local data, we analyze the statistical patterns of local models successively uploaded by a certain client within a certain time span.

Due to the high-dimensional characteristics of local models, it would be difficult to review them directly and the review process would impose a huge computational load on the server. To better analyze the local models, we use PCA to reduce the high-dimensional models to 2-dimensional ones to extract the most useful information. Typical distributions of legitimate and poisoned models after PCA are compared in Figure 7, and the corresponding experimental details can be found in section VI.

It can be seen that the distribution of poisoned models given by the VagueGAN model is very close to those of legitimate

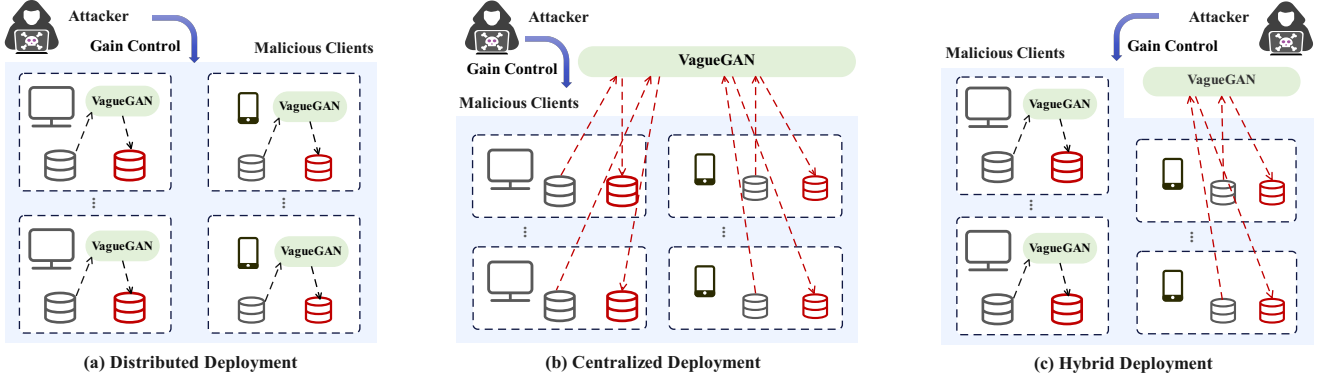


Fig. 6: Three ways to deploy VagueGAN

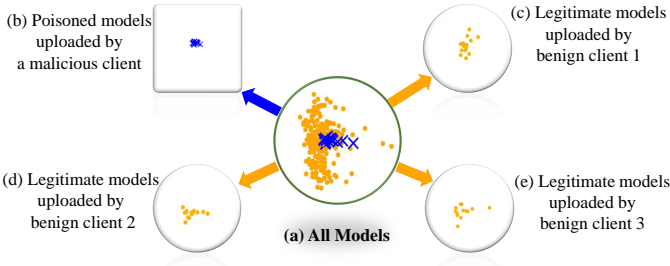


Fig. 7: Legitimate and poisoned models after PCA

models except for their distribution density or consistency levels. The poisoned models uploaded by the same malicious client are more densely distributed within a smaller region. This is mainly caused by the consistency of GAN outputs, as GAN-generated data usually have a certain degree of data feature similarity. Malicious clients keep using similar GAN-poisoned data train poisoned models, and the consistency of GAN outputs further leads to the consistency of the corresponding poisoned models. Inspired by this observation, we propose to identify malicious clients by examining the consistency level of local models successively uploaded by every client.

B. MCD Design

We propose a new defense method named Model Consistency-Based Defense (MCD), which is performed by the server in four steps. The specific process is as follows:

a) Step 1 Model Processing: MCD maintains a trusted set of clients, denoted as C^{tr} . Here, C^{tr} refers to a collection of clients that are temporarily considered to be benign in the FL system. During the initialization phase, C^{tr} is set to \mathcal{C} . MCD runs periodically for every defense period of T' FL rounds for local model analysis. In each defense period, MCD stores a set $\mathcal{Q}_{f,i}$ of low-dimensional local models uploaded by every trusted client $c_i \in C^{tr}$ to the server in T' rounds, $f = 0, 1, 2, 3, \dots$ stands for the f th defense period, thus $f = \lfloor \frac{t}{T'} \rfloor$. Here we take 2-dimensional models after dimensionality reduction by PCA (as by Equation (9)) as an example, but MCD is not limited to it. In our FL system,

the server randomly selects K out of N clients per round for model aggregation, so $\theta_{t,i}^{(2)} \in \mathcal{Q}_{f,i}$ is set to $NULL$ if client c_i is not selected in round t . MCD identifies malicious clients and removes them from C^{tr} in each defense.

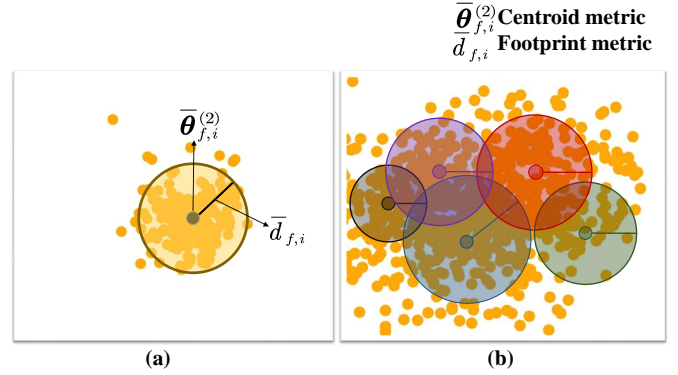


Fig. 8: Two metrics for model consistency evaluation

Afterward, MCD utilizes two crucial metrics calculated from $\mathcal{Q}_{f,i}$ of each trusted client c_i to evaluate a model consistency level. First, for each trusted client c_i , MCD calculates a centroid metric

$$\bar{\theta}_{f,i}^{(2)} = \frac{\sum_{\theta_{t,i}^{(2)} \in \mathcal{Q}_{f,i}} \theta_{t,i}^{(2)}}{|\mathcal{Q}_{f,i}|} \quad (15)$$

where $\bar{\theta}_{f,i}^{(2)}$ represents the center of all models uploaded by a single client c_i (shown in Figure 8(a)). Anomalies with the centroid metric can be used to detect most of the existing data poisoning attacks, such as label flipping attacks, PoisonGAN, noise superimposition attack, etc, as validated in subsection VI-D. Second, MCD calculates a footprint metric

$$\bar{d}_{f,i} = \frac{\sum_{\theta_{t,i}^{(2)} \in \mathcal{Q}_{f,i}} \|\theta_{t,i}^{(2)} - \bar{\theta}_{f,i}^{(2)}\|}{|\mathcal{Q}_{f,i}|} \quad (16)$$

where $\bar{d}_{f,i}$ is the mean of the Euclidean distances, i.e., variances, of all models from the centroid $\bar{\theta}_{f,i}^{(2)}$. A circular region defined by $\bar{\theta}_{f,i}^{(2)}$ as the center and $\bar{d}_{f,i}$ as the radius represents a simplified footprint of the client c_i 's model distribution (shown in Figure 8(a)). Anomalies with the footprint metric can be

Algorithm 2 Client abnormality evaluation algorithm**Input:** Trusted client set \mathcal{C}^{tr} ; baseline client set \mathcal{C}^{base} **Output:** All trusted clients' abnormality set \mathcal{H}_f **Initialization:** Weights of two anomalous terms λ_1, λ_2

```

1: //Calculate Baseline Values
2: for  $c_i \in \mathcal{C}^{base}$  do
3:   Calculate the base value  $\theta_f^{base}$  according to (19)
4:   Calculate the base value  $d_f^{base}$  according to (20)
5: end for
6: //Calculate Abnormal Degree
7: for  $c_i \in \mathcal{C}^{tr}$  do
8:   Calculate the client abnormality  $h_{f,i}$  with  $\lambda_1, \lambda_2$  according to (21)
9:   Get outputted trusted client  $c_i$ 's abnormality  $h_{f,i}$ 
10: end for
11: Output all trusted clients' abnormality set  $\mathcal{H}_f$ 

```

used to detect GAN-based data poisoning attacks when the same GAN model like VagueGAN is applied consistently. Each pair of centroid and footprint metrics is extracted from a set of high-dimensional local models, and MCD can cost-effectively work with such extracted metrics instead of the original models. This greatly saves the storage space of the server, and also keeps the computational effort of MCD low to identify malicious clients.

Thus far, MCD pre-processes each trusted client c_i 's local models into a pair of two key metrics $(\bar{\theta}_{f,i}^{(2)}, \bar{d}_{f,i})$. Figure 8(b) presents an example of five clients' metric pairs.

b) Step 2 Baseline Value Calculation: MCD calculates baseline values $\theta_f^{base}, d_f^{base}$ of above two metrics for anomaly detection. The calculation of baseline values is a crucial step in MCD as it directly influences the effectiveness of its judgment.

Thus, MCD establishes a baseline client set \mathcal{C}^{base} for baseline values calculation, and the processes of selecting the baseline clients are as follows. Firstly, MCD maintains a first baseline client (for instance, the server acts as a such client to train a local model). This client is considered 100% secure and immune to attacks, and its model metrics are denoted as $(\hat{\theta}_f^{(2)}, \hat{d}_f)$. The first baseline client can expand to multiple ones if possible. Secondly, MCD defines \mathcal{C}^{base} as the set of baseline clients whose model metrics are within a neighborhood of those of the first baseline client. Two constants Ω_1, Ω_2 are used to define the size of the neighborhood:

$$\frac{\|\bar{\theta}_{f,i}^{(2)} - \hat{\theta}_f^{(2)}\|}{\hat{d}_f} < \Omega_1 \quad (17)$$

which represents the requirement for the centroid metrics, and

$$\frac{|\bar{d}_{f,i} - \hat{d}_f|}{\hat{d}_f} < \Omega_2 \quad (18)$$

which represents the requirement for the footprint metrics.

After filtering out the baseline client set \mathcal{C}^{base} based on the above constraints, MCD utilizes the model metrics of

the baseline clients to calculate the baseline values. The calculation of θ_f^{base} is as follows:

$$\theta_f^{base} = \frac{\sum_{\bar{\theta}_{f,i}^{(2)} \in \mathcal{C}^{base}} \bar{\theta}_{f,i}^{(2)}}{|\mathcal{C}^{base}|} \quad (19)$$

Similarly, the calculation process of d_f^{base} is as follows:

$$d_f^{base} = \frac{\sum_{\bar{d}_{f,i} \in \mathcal{C}^{base}} \bar{d}_{f,i}}{|\mathcal{C}^{base}|} \quad (20)$$

So far, MCD has obtained the centroid baseline value θ_f^{base} and the footprint baseline value d_f^{base} .

c) Step 3 Client Abnormality Calculation: MCD uses the baseline values to calculate every trusted client abnormality separately. That is to calculate the degree of deviation of each client c_i 's metric pair $(\bar{\theta}_{f,i}^{(2)}, \bar{d}_{f,i})$ from the baseline values. MCD quantifies it as $h_{f,i}$, and the calculation of $h_{f,i}$ is:

$$h_{f,i} = \lambda_1 \left(\frac{\|\bar{\theta}_{f,i}^{(2)} - \theta_f^{base}\|}{d_f^{base}} \right) + \lambda_2 (|d_f^{base} - \bar{d}_{f,i}|) \quad (21)$$

The client abnormality set of all trusted clients is denoted as \mathcal{H}_f . The first part of $h_{f,i}$ can be used to detect anomalies with the centroid metric, while the second part can be used to detect anomalies with the footprint metric. λ_1, λ_2 are weights and can be set as needed. The first half and the second half of Equation (21) are not of the same order of magnitude. λ_1 and λ_2 are used to normalize the two parts. The steps for client abnormality evaluation are summarized in Algorithm 2.

d) Step 4 Malicious Client Identification: After obtaining all trusted client abnormality values, MCD finds a median value say h_f^{med} . MCD then calculates an abnormality threshold h_f^{thr} for malicious client detection:

$$h_f^{thr} = \delta h_f^{med} \quad (22)$$

where parameter $\delta \in (1, 3)$ controls the threshold. MCD then marks every client with an client abnormality larger than the threshold as a malicious client. If MCD detects a malicious client, it will be removed from the trusted client set \mathcal{C}^{tr} . The complete procedure of MCD, executed by the server, is outlined in Algorithm 3.

Overall, MCD can be implemented in a cost-effective manner. MCD operates without model collection overhead, since it directly reuses the local models already collected by the server for federated aggregation. Furthermore, on the premise of ensuring that the accuracy of judgment is not affected, some measures have been taken to ensure minimum impact on the server load: (1) MCD works with extracted metrics instead of original high-dimensional models, which avoids high space load on the server. (2) MCD uses a lightweight anomaly detection algorithm, which does not require complex computations. (3) MCD defenses every period of tens of training rounds rather than every round, which avoids high computational load on the server.

VI. PERFORMANCE EVALUATION

In this section, we evaluate our VagueGAN and MCD through extensive experiments on multiple real-world datasets.

Algorithm 3 MCD defense algorithm

Input: All clients' model set $\mathcal{Q}_f = \{\mathcal{Q}_{f,1}, \mathcal{Q}_{f,2}, \dots, \mathcal{Q}_{f,i}, \dots, \mathcal{Q}_{f,N}\}$

Output: Trusted client set \mathcal{C}^{tr}

Initialization: Defense period of MCD T' ; Trusted client set $\mathcal{C}^{tr} = \mathcal{C}$

- 1: **for** $t = 1, 2, \dots, T$ **do**
- 2: **if** $t \% T' = 0$ **then**
- 3: $f = \lfloor \frac{t}{T'} \rfloor$
- 4: **for** $\mathcal{Q}_{f,i} \in \mathcal{Q}_f$ **do**
- 5: Calculate model metrics $\bar{\theta}_{f,i}^{(2)}, \bar{d}_{f,i}$ according to (15),(16)
- 6: Use $(\bar{\theta}_{f,i}^{(2)}, \bar{d}_{f,i})$ instead of $\mathcal{Q}_{f,i}$
- 7: **end for**
- 8: Select baseline client set \mathcal{C}^{base} according to (17)(18)
- 9: Run Algorithm 2: Client abnormality evaluation
- 10: Get outputted \mathcal{H}_f
- 11: Calculate h_f^{thr} according to (22)
- 12: **for** $c_i \in \mathcal{C}^{tr}$ **do**
- 13: **if** $h_{f,i} > h_f^{thr}$ **then**
- 14: remove c_i from \mathcal{C}^{tr}
- 15: remove $\mathcal{Q}_{f,i}$ from \mathcal{Q}_f
- 16: **end if**
- 17: **end for**
- 18: **end if**
- 19: Update $\mathcal{C}^{tr}, \mathcal{Q}_f$
- 20: **end for**

A. Experimental Settings

TABLE I: Details of datasets

| Dataset | Data Size | Labels | Training Samples | Testing Samples |
|----------|-----------|--------|------------------|-----------------|
| MNIST | (28,28,1) | 10 | 60000 | 10000 |
| F-MNIST | (28,28,1) | 10 | 60000 | 10000 |
| CIFAR-10 | (32,32,3) | 10 | 50000 | 10000 |

a) Datasets and Learning Task: We take image data as an example to evaluate the poisoning capability of our VagueGAN, but the idea of “vague data” is not limited to this specific data type. We conduct our experiments on three typical real-world datasets, which are MNIST [39], Fashion-MNIST [40] and CIFAR-10 [41]. These datasets are also commonly used in existing work. Details of these datasets are shown in Table I. The learning task of our FL system is to train a deep learning model for image classification. In the experiments using MNIST and Fashion-MNIST, a convolutional neural network (CNN) with two convolutional layers and batch normalization has been deployed. In the experiments using CIFAR-10, a CNN with six convolutional layers, batch normalization, and two fully connected layers has been implemented.

b) Federated Learning Setup: We utilize the Pytorch package to implement FL in Python. The FL system consists of $N = 60$ clients by default and a central server, which randomly chooses $K = 10$ clients per round for model aggregation. Each training process of FL lasts $T = 200$ rounds. Each training dataset is split into N partitions as the clients' local datasets, which can be either independent and identically distributed (IID) or non-IID. The non-IID case is set according to [42].

c) Attack Methods: The four data poisoning attack methods in comparison are set up as follows.

(1) *Label flipping attack* [8]: This method flips specific labels of training data to achieve targeted data poisoning in FL. Specifically, the attacker poisons a local dataset as follows: For all samples belonging to a source class, change their labels to another target class. In our experiment, every data sample with label “6” is given a poisoned label “0”.

(2) *Label flipping attack with PoisonGAN* [9]: A label flipping attack can work with PoisonGAN, an off-the-shelf GAN model used to enlarge the sizes of local datasets with legitimate pseudo samples by using a discriminator initialized by the global model. Note that PoisonGAN is just a data augmentation method used to enhance the label flipping attack, and it does not directly generate poisoned data. In our experiment, the malicious clients first enlarge their local datasets with pseudo data generated by PoisonGAN and then carry out a label flipping attack as above. The amount of pseudo data generated by PoisonGAN is 10% of each local dataset.

(3) *Noise superimposition attack:* The attacker superimposes a certain type of noise on real data to generate poisoned data. Either light or heavy Gaussian noise is directly added to the original data, where light noise is with mean = 0 and variance = 0.1; heavy noise is with mean = 0 and variance = 0.3. In addition, SAP noise is added similarly, where 30% pixels of each image sample are noise-superimposed, and the proportion of “salt” versus “pepper” noise is 0.5.

(4) *VagueGAN:* For our VagueGAN, it generates the same amount of poisoned data as the real data, and replaces all the real data with the poisoned data. By default, let $\kappa = 0.2$, $E = 600$.

d) Defense Methods: In response to the above four data poisoning attacks, we compare the following three defense methods.

(1) *PCA* [8]: This method constructs a local model list on the server, collecting all local models used for federated aggregation. After the local model list is constructed across $T' = 80$ rounds, it is standardized by zeroing the mean and being scaled to unit variance. The standardized list is fed into PCA for dimensionality reduction and visualization, and then clients with large outliers are labeled as malicious and subsequently ignored.

(2) *UMAP* [12]: This method follows the same logic as the PCA, except for using UMAP for dimensionality reduction. As for its settings, the neighborhood size for local structure approximation is 200, layout control parameter is 0.8, and cosine distance is computed in the ambient space of input data.

TABLE II: Test accuracy in presence of data poisoning attacks (%)

| Client data distribution | IID | | | | | non-IID | | | | |
|-----------------------------|---------------------------------------|-------|-------|-------|-------|---------|-------|-------|-------|-------|
| | Malicious Clients Percentage α | | | | | | | | | |
| | 0% | 5% | 10% | 20% | 30% | 0% | 5% | 10% | 20% | 30% |
| MNIST | | | | | | | | | | |
| Label Flipping | 98.73 | 98.65 | 98.48 | 98.32 | 98.11 | 98.39 | 98.32 | 98.08 | 97.92 | 97.59 |
| Label Flipping+PoisonGAN | 98.73 | 98.64 | 98.43 | 98.21 | 98.04 | 98.39 | 98.3 | 97.91 | 97.88 | 97.44 |
| Light Noise Superimposition | 98.73 | 98.66 | 98.57 | 98.41 | 98.31 | 98.39 | 98.37 | 98.15 | 98.02 | 97.74 |
| Heavy Noise Superimposition | 98.73 | 98.63 | 98.49 | 98.37 | 98.11 | 98.39 | 98.36 | 98.03 | 97.89 | 97.61 |
| SAP Noise Superimposition | 98.73 | 98.70 | 98.62 | 98.56 | 98.43 | 98.39 | 98.37 | 98.19 | 98.04 | 97.82 |
| VagueGAN | 98.73 | 98.61 | 98.35 | 97.84 | 97.46 | 98.39 | 98.13 | 97.94 | 97.77 | 97.37 |
| Fashion-MNIST | | | | | | | | | | |
| Label Flipping | 87.97 | 87.73 | 87.20 | 86.01 | 85.48 | 87.25 | 86.73 | 86.18 | 85.31 | 84.36 |
| Label Flipping+PoisonGAN | 87.97 | 87.59 | 87.17 | 85.77 | 85.09 | 87.25 | 86.59 | 86.01 | 85.04 | 84.08 |
| Light Noise Superimposition | 87.97 | 87.81 | 87.58 | 86.92 | 86.57 | 87.25 | 87.08 | 86.82 | 86.29 | 85.72 |
| Heavy Noise Superimposition | 87.97 | 87.71 | 87.15 | 86.16 | 85.56 | 87.25 | 86.94 | 86.57 | 85.83 | 85.33 |
| SAP Noise Superimposition | 87.97 | 87.80 | 87.52 | 86.99 | 86.43 | 87.25 | 87.12 | 86.77 | 86.32 | 85.94 |
| VagueGAN | 87.97 | 87.34 | 86.79 | 85.87 | 84.77 | 87.25 | 86.64 | 85.84 | 84.91 | 84.02 |
| CIFAR-10 | | | | | | | | | | |
| Label Flipping | 76.28 | 75.69 | 74.99 | 73.86 | 72.85 | 73.61 | 72.32 | 71.23 | 70.18 | 68.78 |
| Label Flipping+PoisonGAN | 76.28 | 75.62 | 74.84 | 73.77 | 72.66 | 73.61 | 72.16 | 71.06 | 70.04 | 68.66 |
| Light Noise Superimposition | 76.28 | 76.03 | 75.71 | 74.93 | 74.07 | 73.61 | 72.94 | 72.03 | 71.26 | 70.53 |
| Heavy Noise Superimposition | 76.28 | 75.88 | 75.13 | 74.24 | 73.11 | 73.61 | 72.82 | 71.88 | 70.73 | 69.94 |
| SAP Noise Superimposition | 76.28 | 76.12 | 75.73 | 74.71 | 73.96 | 73.61 | 72.99 | 71.97 | 71.22 | 70.38 |
| VagueGAN | 76.28 | 74.94 | 74.02 | 73.16 | 71.93 | 73.61 | 71.96 | 70.64 | 69.55 | 67.79 |

(3) *MCD*: For our MCD parameters are set as follows. In MCD, the magnitude of the first part of $h_{f,i}$ in (21) is slightly larger than that of the second part. To balance the two anomaly evaluation components, we set $\lambda_1 = 1$, $\lambda_2 = 2$. The number of FL rounds for a defense period is $T' = 80$. The constraints on the neighborhood for C^{base} are $\Omega_1=4$, $\Omega_2=2$.

B. Attack Performance Comparison

In this subsection, we evaluate and compare the three attack methods in the same scenario, all of which are implemented to poison the same local datasets.

a) *Effectiveness of Poisoning Attacks*: The attack effectiveness of data poisoning here is characterized by the global model accuracy a_t^p in presence of an attack, under the same setting with the same no-attack accuracy a_t . With the percentage of malicious clients α ranged from 5% to 30%, the effectiveness of the three attack methods is compared in Table II, and the results are averaged after 10 runs. Compared with the benchmark methods, our VagueGAN mostly achieves better attack effectiveness, though its major advantage is the trade-off between attack effectiveness and stealthiness. Not surprisingly, increasing percentage of malicious clients and a non-IID setting lower the global model accuracy. In addition, the attack methods perform differently on different datasets. Compared with Fashion-MNIST and MNIST, CIFAR-10 is more vulnerable to data poisoning attacks. To explain, we name the rounds in which the number of malicious clients selected by the server is greater than 2 as abnormal rounds, and the rest of the rounds as normal rounds. We find that after any abnormal round, the accuracy rate of the global model generally first decreases, and then returns to normal after a few normal rounds. In comparison, more such normal rounds are needed for CIFAR-10 than Fashion-MNIST and MNIST. This is because CIFAR-10 can make FL tasks more complex and thus lead to more normal rounds for a recovery.

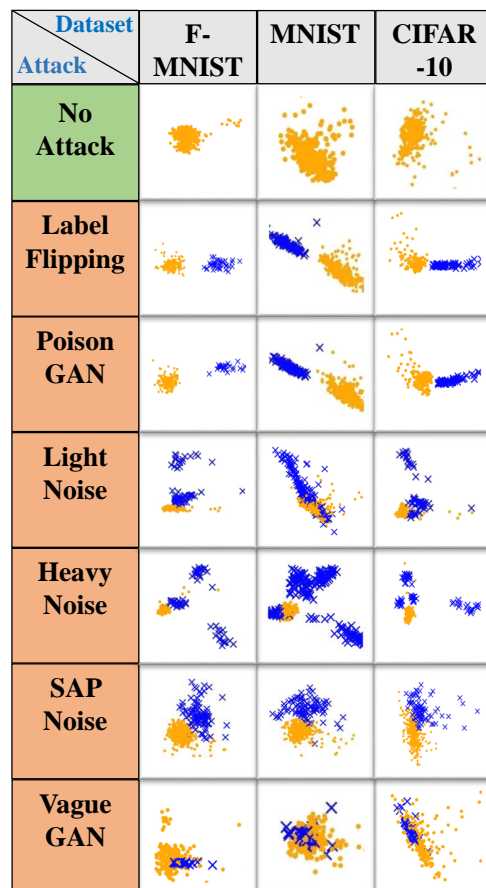


Fig. 9: Two-dimensional local model visualization

b) *Stealthiness of Poisoning Attacks*: First, the attack stealthiness of data poisoning is characterized by the statistical distances between legitimate and poisoned models obtained after applying e.g., PCA. Most of the existing defense methods

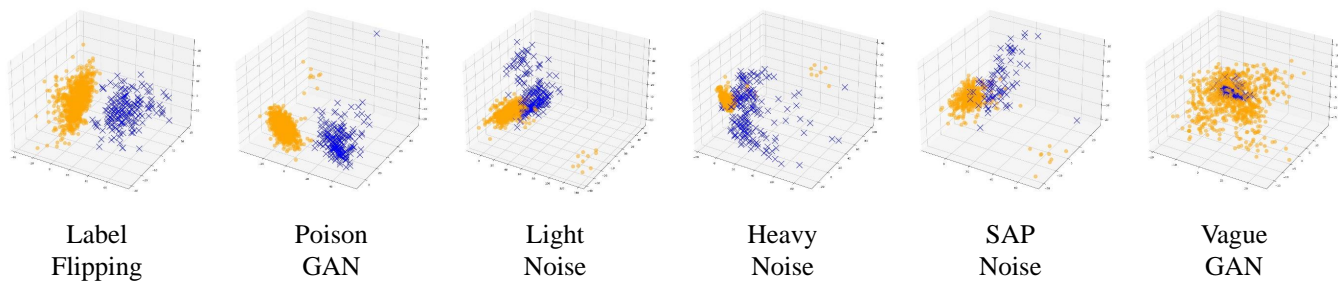


Fig. 10: Three-dimensional local model visualization

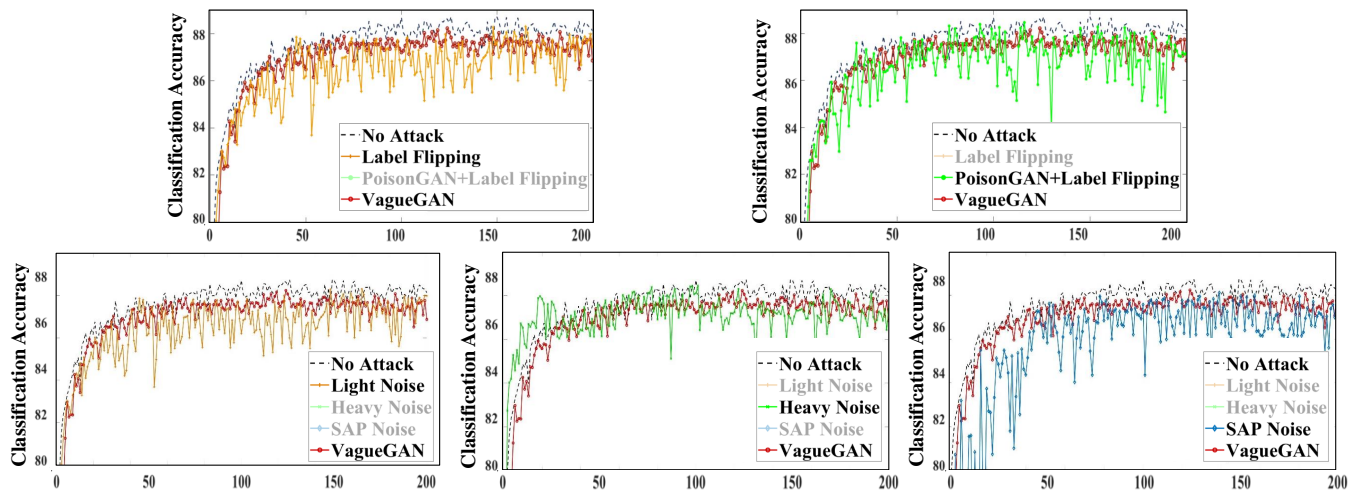
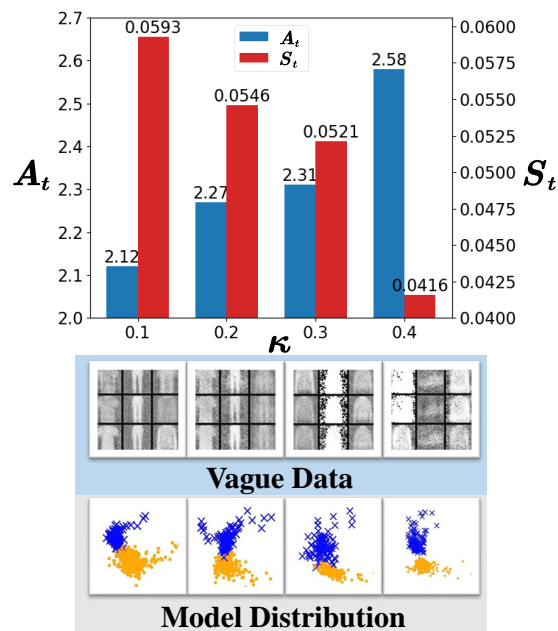


Fig. 11: VagueGAN versus label flipping and noise superimposition accuracy fluctuations

follow a similar idea. Take the Fashion-MNIST task under the setting of IID and $\alpha = 20\%$ as an example. After compressing local models to 2-dimensional for visualization using PCA, as shown in Figure 9, the statistical distance between legitimate models (yellow Os for the last 50 rounds) and poisoned models (blue Xs) can be measured. Similarly, the local models can also be visualized in 3-dimensional using PCA, as shown in Figure 10. Clearly in both 2- and 3-dimensional, our VagueGAN achieves much better attack stealthiness than the benchmark methods. The existing data poisoning attacks cannot be successful as long as a PCA-based defense method is enabled, but our VagueGAN poisoning attack is much harder to detect.

Second, the attack stealthiness of data poisoning can also be characterized by fluctuations in the global model accuracy a_t^p . Such accuracy fluctuations are linked to attack stealthiness because the server’s random selection of clients per round may bring more or less possibly noticeable poisoned models and thus may cause the accuracy fluctuations. Taking the Fashion-MNIST task under the setting of IID and $\alpha = 20\%$ as an example, the accuracy level fluctuating with FL rounds given by VagueGAN versus other data poisoning attack methods is shown in Figure 11. Clearly, our VagueGAN with small accuracy fluctuations mostly approximates the no attack case, but the benchmark methods result in relatively large accuracy fluctuations and are easily detectable even without statistical

Fig. 12: Impact of suppression factor κ

analysis. Therefore, excellent stealthiness of VagueGAN poisoning attack makes it easier to be successful.

TABLE III: MCD detection metrics in the label flipping attack scenario

| i | 0 | 1 | 2 | 3 | 4 | 5 | 6 | 7 | 8 | 9 | |
|----------------------------|----------------|----------------|----------------|----------------|----------------|----------------|----------------|----------------|----------------|----------------|------------------------------------|
| $\bar{\theta}_{f,i}^{(2)}$ | (-6.22, 4.26) | (21.87, -0.58) | (-1.86, -9.85) | (-2.67, 11.74) | (-3.58, 3.63) | (-4.64, -3.19) | (-7.15, 0.66) | (-6.87, -3.16) | (-4.59, -2.59) | (23.13, 5.61) | $\theta_f^{base} = (-5.31, -0.62)$ |
| $\bar{d}_{f,i}$ | 4.09 | 3.07 | 3.79 | 3.13 | 4.44 | 3.09 | 3.43 | 2.85 | 3.20 | 3.14 | |
| $h_{f,i}$ | 1.49 | 8.74 | 2.97 | 4.18 | 1.38 | 1.26 | 0.67 | 1.84 | 0.87 | 9.13 | |
| i | 10 | 11 | 12 | 13 | 14 | 15 | 16 | 17 | 18 | 19 | |
| $\bar{\theta}_{f,i}^{(2)}$ | (21.51, -4.57) | (-5.27, 1.53) | (-3.44, -7.33) | (-5.83, 2.51) | (-4.82, -1.70) | (-7.19, -6.73) | (-8.05, -6.00) | (-4.93, 0.06) | (-7.89, 0.25) | (22.01, -0.43) | $d_f^{base} = 3.32$ |
| $\bar{d}_{f,i}$ | 4.45 | 3.92 | 3.03 | 3.30 | 2.84 | 2.78 | 2.82 | 2.97 | 2.25 | 3.43 | |
| $h_{f,i}$ | 8.17 | 0.65 | 2.67 | 0.99 | 1.34 | 3.26 | 2.82 | 0.93 | 2.95 | 8.23 | |

C. Performance Trade-off Analysis

As discussed in subsection IV-C, a balanced trade-off between attack effectiveness A_t and stealthiness S_t can be achieved by setting the values of κ and E appropriately.

a) **Generator suppression factor κ** : The value of κ can be adjusted to limit the generation ability of the generator of VagueGAN. Taking the Fashion-MNIST task under the setting of IID, $\alpha = 20\%$, and $E = 400$ as an example, the impact of κ on the trade-off between A_t and S_t is evaluated in Figure 12. It can be seen that increasing κ from 0.1 to 0.4 gives increasing A_t but decreasing S_t . To ensure a not easily detectable attack, a reasonable value of κ , e.g., 0.2, should not be too large.

b) **Number of training epochs E** : The value of E can be set to control the fitting state of VagueGAN. When $\alpha = 20\%$, the impact of E on the trade-off between A_t and S_t is evaluated in Figure 13. It can be seen that with the increase of E , effectiveness A_t gradually decreases, while stealthiness S_t gradually increases. The rate of change for both A_t and S_t decreases with the increase of E . On the one hand, the value of E cannot be too small. We find that according to the visualized model distribution, when $S_t < 0.05$, the corresponding data poisoning attack will become detectable. Although the performance of A_t is satisfactory at this time, the attack cannot be successful if given a regular defense system. On the other hand, the value of E cannot be too large. For the Fashion-MNIST task as an example, we find that the vague data generated by VagueGAN will be no longer “vague” when $E > 600$ and the quality of vague data will no longer change when $E > 1000$. For this case, the performance of A_t can be overly harmed. More generally, we find that an appropriate value of E can be $0.5e_{lim}$, where e_{lim} is the number of training epochs required for VagueGAN to reach a converged steady state, e.g., $e_{lim} = 600$ for MNIST, 1000 for Fashion-MNIST, and 1600 for CIFAR-10.

D. Comparison of supervised and unsupervised VagueGANs

In this subsection, we present an experimental comparison of supervised VagueGAN with its unsupervised variant. We evaluate their time overhead, attack effectiveness, and stealthiness with the same settings as follows: generator suppression factor $\kappa=0.2$; the number of training epochs E are taken as 200, 400, 600, and 800, respectively; and the same amount of poisoned data is generated.

Firstly, the time overheads are compared for the two VagueGANs on the same experimental device, with a GPU:RTX

3090(24GB) and a CPU:12 vCPU Intel(R) Xeon(R) Platinum 8255C CPU @ 2.50GHz. Figure 14(a) illustrates that the time overhead of unsupervised VagueGAN is greater than that of supervised VagueGAN. Furthermore, the larger the number of training epochs, the greater the discrepancy between the two can be observed. This is due to the necessity that unsupervised VagueGAN maintains an additional classifier, Q , and learns the auxiliary features of the training data.

Secondly, we compare the attack effectiveness of two VagueGANs. Figure 14(b) demonstrates that both VagueGANs exhibit excellent, comparable attack effectiveness. It is noteworthy that the unsupervised attack is more stable and less susceptible to fluctuations in training epochs.

Finally, we compare the attack stealthiness of the two VagueGANs. As illustrated in Figure 15, the outcomes are compared under the trade-off between effectiveness and stealthiness ($\kappa = 0.2, E = 600$), indicating excellent stealthiness. Furthermore, it is evident that both VagueGANs not only harm the global model performance but also indirectly mislead the distribution of some benign client models and make them look like outliers.

E. Defense Performance Comparison

In this subsection, we evaluate the effectiveness of MCD against different data poisoning attacks in FL systems, including label flipping attack, label flipping attack with PoisonGAN, noise superimposition attack and VagueGAN. The FL system is set as follows: the total number of clients $N = 20$; the number of clients selected by the server in each round $K = 5$; the number of FL training rounds $T = 200$; the main task dataset is Fashion-MNIST under the setting of IID. We experiment a case where the percentage of malicious clients α is 20%.

a) **Anomaly detection capability of MCD**: Tables III-VII are the metric tables of MCD in different attack scenarios. Among them, each red client represents a malicious client, and the green client represents the pre-baseline client.

Table III and Table IV present the results of the label flipping attacks and label flipping attacks with PoisonGAN, respectively. It is evident from these two tables that the $\bar{\theta}_{f,i}^{(2)}$ of the malicious clients exhibit pronounced anomalies in both attack scenarios. The results shown in Tables V indicate that the abnormal behavior of the light noise superimposition attack is similar to that of label flipping attack, as both exhibit anomalies in $\bar{\theta}_{f,i}^{(2)}$. In the scenario of heavy noise and SAP

TABLE IV: MCD detection metrics in the label flipping attack with PoisonGAN scenario

| i | 0 | 1 | 2 | 3 | 4 | 5 | 6 | 7 | 8 | 9 | $\theta_f^{base} =$ $(-4.57, 0.44)$ $d_f^{base} =$ 4.15 |
|----------------------------|----------------|----------------|----------------|---------------|---------------|----------------|----------------|----------------|----------------|---------------|--|
| $\bar{\theta}_{f,i}^{(2)}$ | (19.61, -0.24) | (-4.49, -0.33) | (21.47, -0.52) | (-4.73, -2.7) | (-2.09, 3.05) | (-5.24, -1.12) | (-3.13, 1.56) | (-3.22, 6.41) | (-6.38, 4.06) | (-5.93, 0.64) | |
| $\bar{d}_{f,i}$ | 3.68 | 5.33 | 3.06 | 4.46 | 4.62 | 5.10 | 4.02 | 4.09 | 4.48 | 3.60 | |
| $h_{f,i}$ | 6.77 | 2.55 | 8.46 | 1.38 | 1.81 | 2.31 | 0.70 | 1.59 | 1.64 | 1.43 | |
| i | 10 | 11 | 12 | 13 | 14 | 15 | 16 | 17 | 18 | 19 | |
| $\bar{\theta}_{f,i}^{(2)}$ | (22.25, -0.53) | (21.66, -0.57) | (-3.95, 2.86) | (-5.07, 1.43) | (-6.55, 4.28) | (-5.73, -1.12) | (-3.94, -2.67) | (-3.32, -5.79) | (-4.29, -5.14) | (-4.98, 1.64) | |
| $\bar{d}_{f,i}$ | 3.31 | 2.98 | 4.03 | 4.25 | 4.69 | 4.32 | 4.01 | 4.22 | 4.12 | 4.65 | |
| $h_{f,i}$ | 8.15 | 8.67 | 0.84 | 0.47 | 1.94 | 0.81 | 1.04 | 1.71 | 1.56 | 1.31 | |

TABLE V: MCD detection metrics in the light noise superimposition attack scenario

| i | 0 | 1 | 2 | 3 | 4 | 5 | 6 | 7 | 8 | 9 | $\theta_f^{base} =$ $(-1.15, 0.25)$ $d_f^{base} =$ 2.72 |
|----------------------------|---------------|---------------|----------------|---------------|---------------|----------------|-----------------|----------------|---------------|---------------|--|
| $\bar{\theta}_{f,i}^{(2)}$ | (3.35, 10.36) | (-0.40, 1.20) | (2.66, 2.45) | (8.81, 2.52) | (-1.10, 0.05) | (-3.96, -2.02) | (13.32, -26.22) | (-3.05, 0.80) | (1.40, -3.55) | (-1.07, 1.17) | |
| $\bar{d}_{f,i}$ | 3.89 | 2.53 | 2.91 | 5.08 | 1.71 | 2.02 | 4.04 | 3.88 | 2.37 | 3.90 | |
| $h_{f,i}$ | 6.41 | 0.82 | 2.00 | 8.48 | 2.10 | 2.73 | 13.71 | 3.05 | 2.38 | 2.70 | |
| i | 10 | 11 | 12 | 13 | 14 | 15 | 16 | 17 | 18 | 19 | |
| $\bar{\theta}_{f,i}^{(2)}$ | (-4.34, 3.92) | (-3.22, 1.31) | (-0.76, -1.64) | (-1.50, 0.18) | (-2.14, 2.11) | (0.37, -1.00) | (2.60, 1.76) | (-1.63, -3.89) | (-2.33, 1.20) | (4.27, 12.33) | |
| $\bar{d}_{f,i}$ | 2.19 | 1.68 | 2.17 | 1.37 | 2.70 | 2.42 | 3.02 | 2.30 | 1.12 | 3.75 | |
| $h_{f,i}$ | 2.81 | 2.94 | 1.81 | 2.83 | 0.82 | 1.32 | 2.09 | 2.35 | 1.12 | 6.89 | |

TABLE VI: MCD detection metrics in the heavy noise superimposition attack scenario

| i | 0 | 1 | 2 | 3 | 4 | 5 | 6 | 7 | 8 | 9 | $\theta_f^{base} =$ $(-0.51, -0.62)$ $d_f^{base} =$ 0.82 |
|----------------------------|----------------|----------------|---------------|----------------|-----------------|---------------|----------------|------------------|----------------|----------------|---|
| $\bar{\theta}_{f,i}^{(2)}$ | (-0.81, -1.72) | (0.01, -0.86) | (0.40, 0.01) | (-0.30, 0.09) | (32.10, -10.60) | (0.83, -1.00) | (-0.87, -0.68) | (-22.62, -19.32) | (-7.12, 28.24) | (-1.79, -0.92) | |
| $\bar{d}_{f,i}$ | 0.73 | 0.75 | 0.76 | 0.93 | 6.22 | 0.69 | 0.80 | 6.18 | 5.86 | 0.78 | |
| $h_{f,i}$ | 1.48 | 0.77 | 1.41 | 1.01 | 46.98 | 1.83 | 0.46 | 40.68 | 41.15 | 1.64 | |
| i | 10 | 11 | 12 | 13 | 14 | 15 | 16 | 17 | 18 | 19 | |
| $\bar{\theta}_{f,i}^{(2)}$ | (0.11, -0.87) | (-0.88, -0.56) | (4.70, 14.92) | (-0.70, -1.48) | (0.06, -0.57) | (0.31, -0.26) | (-0.95, -0.48) | (-1.39, 0.67) | (-1.13, -0.28) | (-1.09, -1.00) | |
| $\bar{d}_{f,i}$ | 1.03 | 0.85 | 4.92 | 0.68 | 0.79 | 0.83 | 0.82 | 0.90 | 0.74 | 1.05 | |
| $h_{f,i}$ | 1.03 | 0.48 | 24.09 | 1.21 | 0.73 | 1.11 | 0.56 | 1.92 | 0.95 | 1.07 | |

TABLE VII: MCD detection metrics in the SAP noise superimposition attack scenario

| i | 0 | 1 | 2 | 3 | 4 | 5 | 6 | 7 | 8 | 9 | $\theta_f^{base} =$ $(-0.75, -3.70)$ $d_f^{base} =$ 1.50 |
|----------------------------|----------------|-----------------|----------------|----------------|----------------|----------------|----------------|----------------|----------------|----------------|---|
| $\bar{\theta}_{f,i}^{(2)}$ | (-2.32, -2.46) | (-13.38, 14.01) | (0.28, -6.14) | (1.23, -5.05) | (-1.61, -0.55) | (-3.28, -2.26) | (-1.55, -2.85) | (-0.41, -3.78) | (-12.11, 8.79) | (-1.81, -3.06) | |
| $\bar{d}_{f,i}$ | 1.90 | 3.06 | 1.38 | 1.41 | 2.42 | 1.62 | 1.56 | 1.20 | 2.60 | 1.12 | |
| $h_{f,i}$ | 2.8 | 24.82 | 2.88 | 2.57 | 5.1 | 3.15 | 1.28 | 0.9 | 19.09 | 1.99 | |
| i | 10 | 11 | 12 | 13 | 14 | 15 | 16 | 17 | 18 | 19 | |
| $\bar{\theta}_{f,i}^{(2)}$ | (35.53, 9.16) | (2.88, -6.84) | (-1.02, -3.27) | (-0.56, -2.42) | (-1.74, -4.62) | (-1.98, -2.45) | (-3.64, 24.99) | (0.42, -6.47) | (0.13, -2.96) | (-0.58, -4.17) | |
| $\bar{d}_{f,i}$ | 4.52 | 1.01 | 1.24 | 1.18 | 1.20 | 2.52 | 3.87 | 2.05 | 1.05 | 1.20 | |
| $h_{f,i}$ | 44.44 | 5.77 | 1.02 | 1.93 | 1.95 | 3.79 | 33.57 | 4.10 | 2.04 | 1.0 | |

TABLE VIII: MCD detection metrics in the VagueGAN attack scenario

| i | 0 | 1 | 2 | 3 | 4 | 5 | 6 | 7 | 8 | 9 | $\theta_f^{base} =$ $(-0.05, 0.02)$ $d_f^{base} =$ 5.55 |
|----------------------------|---------------|---------------|---------------|---------------|----------------|---------------|----------------|----------------|---------------|---------------|--|
| $\bar{\theta}_{f,i}^{(2)}$ | (-2.52, 0.93) | (-1.95, 1.07) | (-1.62, 0.42) | (-2.77, 4.45) | (-0.19, -2.55) | (0.01, -0.88) | (-0.40, -1.14) | (-2.45, -3.76) | (-2.01, 0.32) | (3.34, -0.24) | |
| $\bar{d}_{f,i}$ | 0.92 | 1.01 | 6.13 | 4.22 | 4.31 | 3.29 | 3.68 | 4.30 | 4.54 | 6.45 | |
| $h_{f,i}$ | 8.92 | 8.64 | 0.32 | 2.81 | 2.12 | 3.49 | 3.11 | 2.51 | 1.35 | 0.66 | |
| i | 10 | 11 | 12 | 13 | 14 | 15 | 16 | 17 | 18 | 19 | |
| $\bar{\theta}_{f,i}^{(2)}$ | (-1.66, 1.02) | (-1.03, 1.21) | (2.19, -0.11) | (2.69, -2.88) | (-0.79, -0.03) | (-0.56, 0.74) | (-1.58, 4.02) | (3.56, 2.36) | (3.80, -3.04) | (2.91, -1.78) | |
| $\bar{d}_{f,i}$ | 1.35 | 6.59 | 8.33 | 6.42 | 4.43 | 5.98 | 1.28 | 5.35 | 6.57 | 8.26 | |
| $h_{f,i}$ | 7.9 | 0.30 | 0.43 | 0.77 | 1.78 | 0.17 | 8.48 | 0.83 | 0.95 | 0.67 | |

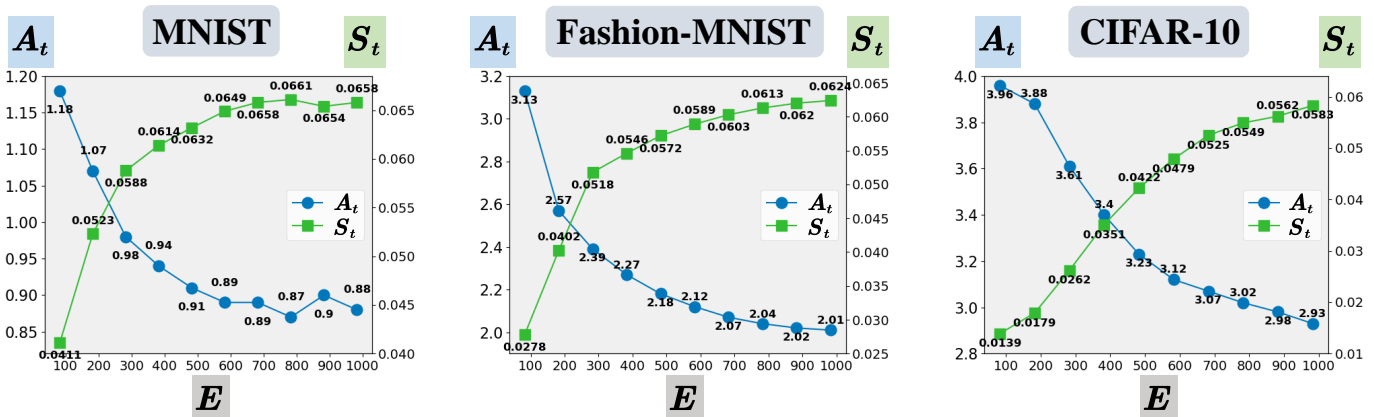
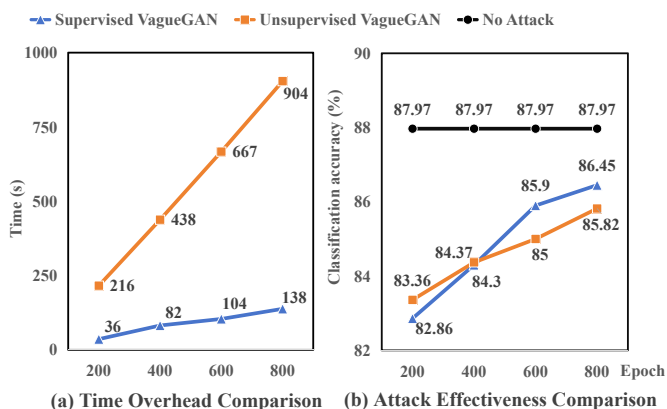
Fig. 13: Impact of VagueGAN training epochs E 

Fig. 14: Supervised vs. unsupervised VagueGAN for time overhead and attack effectiveness

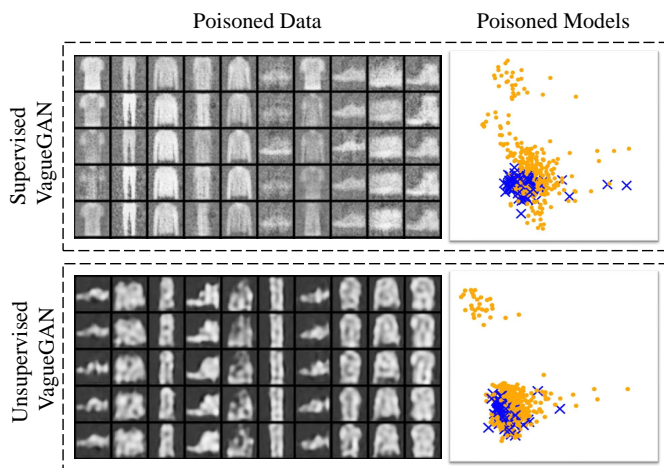


Fig. 15: Supervised vs. unsupervised VagueGAN for attack stealthiness

noise superimposition attack as shown in Tables VI and VII, the malicious clients demonstrate anomalies in both $\bar{\theta}_{f,i}^{(2)}$ and $\bar{d}_{f,i}$, indicating a poor level of stealthiness.

Table VIII displays the judgment results of MCD in the

data poisoning attack scenario based on VagueGAN. Unlike the previous attack scenarios, the malicious clients in the VagueGAN attack scenario exhibit no anomalies in $\bar{\theta}_{f,i}^{(2)}$. This indicates that the malicious clients taking advantage of GAN have largely learned the distribution of legitimate models and thus are hard to detect if using traditional defense methods like PCA. However, the malicious clients exhibit significantly lower $\bar{d}_{f,i}$ values compared with the normal values of benign clients, meaning that MCD still works for GAN-based attacks like VagueGAN.

b) Overall defense effectiveness of MCD: Figure 16 presents the gain in FL performance brought by MCD in six distinct attack scenarios. It is evident that the incorporation of MCD significantly enhances the accuracy of the main task within the FL system. Combining Tables III-VIII to Figure 16 and specific experimental observations, we found across all the six attack scenarios, MCD successfully identifies malicious clients during the first inspection and disregards their subsequent updates (as indicated by the long dashed line). To ensure a stable security level for the FL system, MCD performs regular executions in subsequent training rounds (as indicated by the short dashed line).

We further evaluate MCD in attack scenarios with different proportions of malicious clients, as shown in Table IX. Herein, M denotes the number of malicious clients within the FL system, with M taking values of 1, 2, 4, and 6, corresponding respectively to attack scenarios characterized by α of 5%, 10%, 20%, and 30%. Furthermore, a_t signifies the accuracy of FL system's main task in the absence of malicious clients. Each scenario is performed 10 times for average results. It is shown that MCD can always identify most of the malicious clients as in the upper half table, and thus achieve a gain in FL performance as in the lower half table.

We also compare MCD with PCA and UMAP, two typical existing approaches, as shown in Tables X and XI. The results are produced from the same attack scenarios as Table IX. Each scenario also performed 10 times for average results. It can be seen that MCD always outperforms PCA and UMAP in terms of the number of malicious clients identified and performance improvement, especially under the VagueGAN attack.

In summary, our MCD can effectively work against various

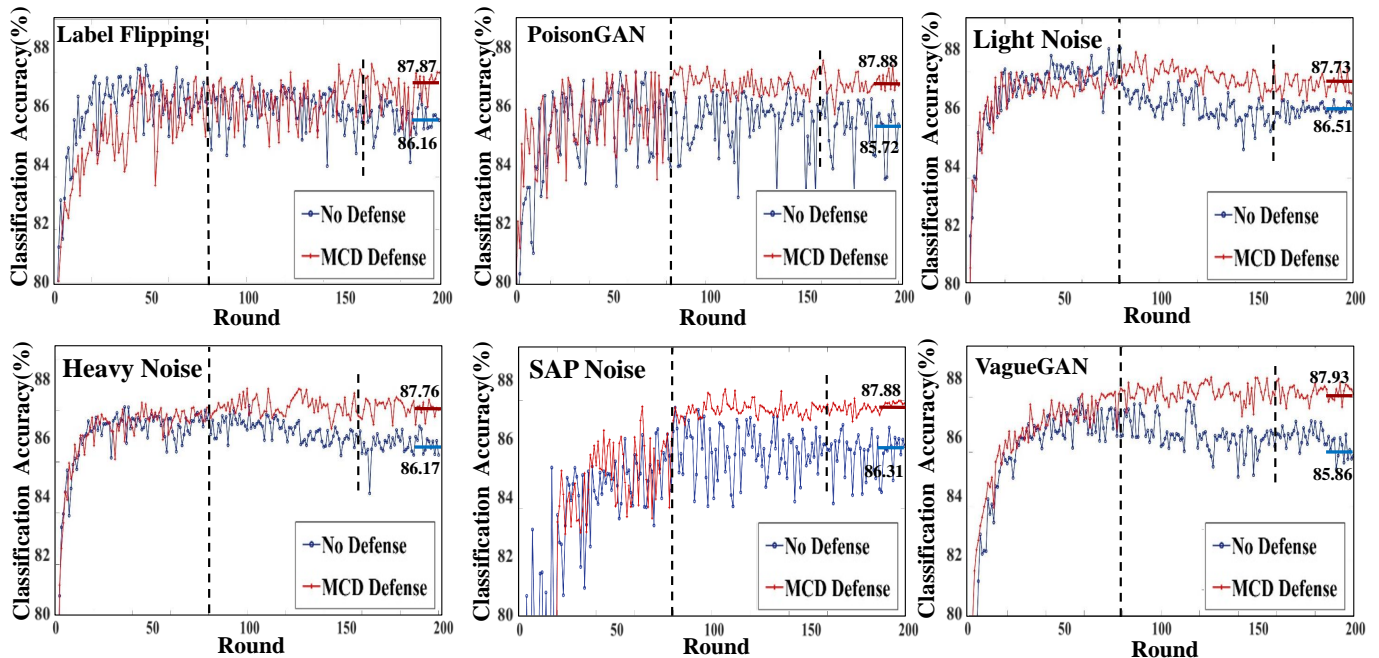


Fig. 16: Defense effectiveness of MCD in different data poisoning attack scenarios

TABLE IX: Defense effectiveness of MCD in different attack scenarios with varying proportions of malicious clients

| | M | α | Label flipping | PoisonGAN | Light noise | Heavy noise | SAP noise | VagueGAN |
|---|-------|----------|--------------------------|--------------------------|--------------------------|--------------------------|--------------------------|--------------------------|
| Number of malicious clients | 1 | 5% | 1 | 1 | 1 | 1 | 1 | 1 |
| detected by MCD (average) | 2 | 10% | 2 | 2 | 1.9 | 2 | 2 | 2 |
| | 4 | 20% | 4 | 4 | 3.8 | 4 | 3.9 | 3.9 |
| | 6 | 30% | 6 | 6 | 5.6 | 6 | 5.7 | 5.8 |
| | a_t | α | Label flipping | PoisonGAN | Light noise | Heavy noise | SAP noise | VagueGAN |
| Main task test accuracy after MCD deployment (average)(%) | 87.97 | 5% | 87.94 (\uparrow 0.21) | 87.92 (\uparrow 0.33) | 87.97 (\uparrow 0.16) | 87.95 (\uparrow 0.24) | 87.95 (\uparrow 0.15) | 87.94 (\uparrow 0.62) |
| | | 10% | 87.91 (\uparrow 0.71) | 87.92 (\uparrow 0.75) | 87.90 (\uparrow 0.32) | 87.87 (\uparrow 0.72) | 87.89 (\uparrow 0.37) | 87.89 (\uparrow 1.11) |
| | | 20% | 87.88 (\uparrow 1.87) | 87.84 (\uparrow 2.07) | 87.87 (\uparrow 0.95) | 87.83 (\uparrow 1.77) | 87.85 (\uparrow 0.86) | 87.86 (\uparrow 1.99) |
| | | 30% | 87.84 (\uparrow 2.36) | 87.80 (\uparrow 2.71) | 87.86 (\uparrow 1.49) | 87.82 (\uparrow 2.26) | 87.90 (\uparrow 1.47) | 87.89 (\uparrow 3.12) |

TABLE X: Defense effectiveness of PCA in different attack scenarios with varying proportions of malicious clients

| | M | α | Label flipping | PoisonGAN | Light noise | Heavy noise | SAP noise | VagueGAN |
|---|-------|----------|--------------------------|--------------------------|--------------------------|--------------------------|--------------------------|--------------------------|
| Number of malicious clients | 1 | 5% | 0.9 | 1 | 0.6 | 0.8 | 0.8 | 0.1 |
| detected by PCA (average) | 2 | 10% | 1.7 | 1.9 | 1.4 | 1.7 | 1.8 | 0.2 |
| | 4 | 20% | 3.5 | 3.6 | 2.7 | 3.5 | 3.6 | 0.6 |
| | 6 | 30% | 5.3 | 5.5 | 4.2 | 5.1 | 5.3 | 0.9 |
| | a_t | α | Label flipping | PoisonGAN | Light noise | Heavy noise | SAP noise | VagueGAN |
| Main task test accuracy after PCA deployment (average)(%) | 87.97 | 5% | 87.92 (\uparrow 0.19) | 87.89 (\uparrow 0.30) | 87.93 (\uparrow 0.12) | 87.92 (\uparrow 0.21) | 87.92 (\uparrow 0.12) | 87.34 (\uparrow) |
| | | 10% | 87.86 (\uparrow 0.66) | 87.87 (\uparrow 0.67) | 87.79 (\uparrow 0.21) | 87.76 (\uparrow 0.61) | 87.78 (\uparrow 0.26) | 86.79 (\uparrow) |
| | | 20% | 87.79 (\uparrow 1.78) | 87.77 (\uparrow 1.76) | 87.71 (\uparrow 0.79) | 87.56 (\uparrow 1.50) | 87.78 (\uparrow 0.79) | 86.01 (\uparrow 0.14) |
| | | 30% | 87.66 (\uparrow 2.18) | 87.61 (\uparrow 2.52) | 87.68 (\uparrow 1.31) | 87.49 (\uparrow 1.93) | 87.82 (\uparrow 1.39) | 84.97 (\uparrow 0.20) |

data poisoning attacks, especially GAN-based ones like our VagueGAN, and can further contribute to FL performance under attacks.

VII. CONCLUSIONS AND FUTURE WORK

In this paper, we have proposed VagueGAN, a GAN model specifically designed for data poisoning attacks against FL systems. Unlike traditional GANs, our VagueGAN has been verified to generate seemingly legitimate vague data with appropriate amounts of poisonous noise. The ways to achieve a balanced trade-off between attack effectiveness and stealthi-

ness have been studied. We have also experimentally demonstrated the distinctiveness of the poisoned data generated by VagueGAN compared to noisy data. Furthermore, we have suggested and verified MCD as a viable countermeasure to VagueGAN if the same GAN model is consistently applied by the attacker.

In the future, we plan to extend our work in two potential directions. The first direction focuses on addressing the limitations of GAN-based attack methods. In particular, the consistency of GAN outputs has been found to be effective in identifying GAN-poisoned data or models. Hence, a future

TABLE XI: Defense effectiveness of UMAP in different attack scenarios with varying proportions of malicious clients

| | M | α | Label flipping | PoisonGAN | Light noise | Heavy noise | SAP noise | VagueGAN |
|--|------------|----------|--------------------------|--------------------------|--------------------------|--------------------------|--------------------------|--------------------------|
| Number of malicious clients | 1 | 5% | 0.7 | 0.8 | 0.4 | 0.8 | 0.8 | 0 |
| detected by UMAP (average) | 2 | 10% | 1.4 | 1.9 | 1.2 | 1.7 | 1.5 | 0 |
| | 4 | 20% | 2.9 | 2.8 | 1.9 | 2.3 | 2.7 | 0.2 |
| | 6 | 30% | 3.3 | 4.0 | 2.9 | 3.7 | 4.1 | 0.7 |
| | α_t | α | Label flipping | PoisonGAN | Light noise | Heavy noise | SAP noise | VagueGAN |
| Main task test accuracy after UMAP deployment (average)(%) | 87.97 | 5% | 87.92 (\uparrow 0.19) | 87.87 (\uparrow 0.28) | 87.93 (\uparrow 0.12) | 87.91 (\uparrow 0.20) | 87.94 (\uparrow 0.14) | 87.34 (\uparrow 0) |
| | | 10% | 87.82 (\uparrow 0.62) | 87.89 (\uparrow 0.69) | 87.79 (\uparrow 0.21) | 87.72 (\uparrow 0.57) | 87.70 (\uparrow 0.18) | 86.79 (\uparrow 0) |
| | | 20% | 87.57 (\uparrow 1.56) | 87.61 (\uparrow 1.60) | 87.59 (\uparrow 0.67) | 87.43 (\uparrow 1.37) | 87.62 (\uparrow 0.63) | 85.96 (\uparrow 0.09) |
| | | 30% | 87.34 (\uparrow 1.86) | 87.39 (\uparrow 2.30) | 87.61 (\uparrow 1.24) | 87.29 (\uparrow 1.73) | 87.60 (\uparrow 1.17) | 84.91 (\uparrow 0.14) |

study can develop more advanced generative models without such a drawback for improved attack stealthiness. The second direction involves further exploration into effective and universally applicable defense mechanisms. Although our MCD has been validated to be useful against GAN-based attacks, the model consistency it relies on may not hold if the attacks are implemented in varying settings. Hence, a future study can produce better adaptive AI-driven techniques for enhanced defense capabilities.

REFERENCES

- [1] Y. Chen, P. Zhu, G. He, X. Yan, H. Baligh, and J. Wu, "From connected people, connected things, to connected intelligence," in *Proc. 6G SUMMIT*, 2020, pp. 1–7.
- [2] N. Rodríguez-Barroso, D. Jiménez-López, M. V. Luzón, F. Herrera, and E. Martínez-Cámara, "Survey on federated learning threats: concepts, taxonomy on attacks and defenses, experimental study and challenges," *Inf. Fusion*, vol. 90, pp. 148–173, 2023.
- [3] L. Lyu, H. Yu, and Q. Yang, "Threats to federated learning: A survey," *arXiv preprint arXiv:2003.02133*, 2020.
- [4] R. Gosselin, L. Vieu, F. Loukil, and A. Benoit, "Privacy and security in federated learning: A survey," *Appl. Sci.*, vol. 12, no. 19, p. 9901, 2022.
- [5] V. Muthukuri, R. M. Parizi, S. Pouriyeh, Y. Huang, A. Dehghantanha, and G. Srivastava, "A survey on security and privacy of federated learning," *Future Gener. Comput. Syst.*, vol. 115, pp. 619–640, 2021.
- [6] M. S. Jere, T. Farnan, and F. Koushanfar, "A taxonomy of attacks on federated learning," *IEEE Security & Privacy*, vol. 19, no. 2, pp. 20–28, 2020.
- [7] G. Xia, J. Chen, C. Yu, and J. Ma, "Poisoning attacks in federated learning: A survey," *IEEE Access*, vol. 11, pp. 10 708–10 722, 2023.
- [8] V. Tolpegin, S. Truex, M. E. Gursoy, and L. Liu, "Data poisoning attacks against federated learning systems," in *Proc. ESORICS*, 2020, pp. 480–501.
- [9] J. Zhang, B. Chen, X. Cheng, H. T. T. Binh, and S. Yu, "Poisoning: Generative poisoning attacks against federated learning in edge computing systems," *IEEE Internet Things J.*, vol. 8, no. 5, pp. 3310–3322, 2020.
- [10] J. Zhang, J. Chen, D. Wu, B. Chen, and S. Yu, "Poisoning attack in federated learning using generative adversarial nets," in *Proc. IEEE TrustCom/BigDataSE*, 2019, pp. 374–380.
- [11] D. Cao, S. Chang, Z. Lin, G. Liu, and D. Sun, "Understanding distributed poisoning attack in federated learning," in *Proc. IEEE ICPADS*, 2019, pp. 233–239.
- [12] D. Upreti, H. Kim, E. Yang, and C. Seo, "Defending against label-flipping attacks in federated learning systems with umap," <https://doi.org/10.21203/rs.3.rs-1984301/v1>, 2022.
- [13] S. Shen, S. Tople, and P. Saxena, "Auror: Defending against poisoning attacks in collaborative deep learning systems," in *Proc. ACM ACSAC*, 2016, pp. 508–519.
- [14] X. Li, Z. Qu, S. Zhao, B. Tang, Z. Lu, and Y. Liu, "Lomar: A local defense against poisoning attack on federated learning," *IEEE Trans. Dependable Secure Comput.*, 2021.
- [15] H. S. Sikandar, H. Waheed, S. Tahir, S. U. Malik, and W. Rafique, "A detailed survey on federated learning attacks and defenses," *Electronics*, vol. 12, no. 2, p. 260, 2023.
- [16] I. Goodfellow, J. Pouget-Abadie, M. Mirza, B. Xu, D. Warde-Farley, S. Ozair, A. Courville, and Y. Bengio, "Generative adversarial networks," *Commun. ACM*, vol. 63, no. 11, pp. 139–144, 2020.
- [17] B. Hitaj, G. Ateniese, and F. Perez-Cruz, "Deep models under the gan: information leakage from collaborative deep learning," in *Proc. ACM CCS*, 2017, pp. 603–618.
- [18] Y. Shi, T. Erpek, Y. E. Sagduyu, and J. H. Li, "Spectrum data poisoning with adversarial deep learning," in *Proc. IEEE MILCOM*, 2018, pp. 407–412.
- [19] H. Huang, J. Mu, N. Z. Gong, Q. Li, B. Liu, and M. Xu, "Data poisoning attacks to deep learning based recommender systems," *arXiv preprint arXiv:2101.02644*, 2021.
- [20] X. Zhang, X. Zhu, and L. Lessard, "Online data poisoning attacks," in *Proc. LADC*, 2020, pp. 201–210.
- [21] A. Schwarzschild, M. Goldblum, A. Gupta, J. P. Dickerson, and T. Goldstein, "Just how toxic is data poisoning? a unified benchmark for backdoor and data poisoning attacks," in *Proc. ICML*, 2021, pp. 9389–9398.
- [22] P. Gupta, K. Yadav, B. B. Gupta, M. Alazab, and T. R. Gadekallu, "A novel data poisoning attack in federated learning based on inverted loss function," *Comput. Secur.*, vol. 130, p. 103270, 2023.
- [23] J. Yang, J. Zheng, T. Baker, S. Tang, Y.-a. Tan, and Q. Zhang, "Clean-label poisoning attacks on federated learning for iot," *Expert Syst.*, vol. 40, no. 5, p. e13161, 2023.
- [24] V. Shejwalkar and A. Houmansadr, "Manipulating the byzantine: Optimizing model poisoning attacks and defenses for federated learning," in *NDSS*, 2021.
- [25] Z. Zhang, X. Cao, J. Jia, and N. Z. Gong, "Fldetector: Defending federated learning against model poisoning attacks via detecting malicious clients," in *Proc. ACM KDD*, 2022, pp. 2545–2555.
- [26] X. Shen, Y. Liu, F. Li, and C. Li, "Privacy-preserving federated learning against label-flipping attacks on non-iid data," *IEEE Internet Things J.*, 2023.
- [27] S. Awan, B. Luo, and F. Li, "Contra: Defending against poisoning attacks in federated learning," in *Proc. ESORICS 2021, Part I 26*, 2021, pp. 455–475.
- [28] Y. Wang, T. Zhu, W. Chang, S. Shen, and W. Ren, "Model poisoning defense on federated learning: A validation based approach," in *Proc. NSS*, 2020, pp. 207–223.
- [29] X. Cao, J. Jia, and N. Z. Gong, "Provably secure federated learning against malicious clients," in *Proc. AAAI*, vol. 35, no. 8, 2021, pp. 6885–6893.
- [30] Y. Zhao, J. Chen, J. Zhang, D. Wu, M. Blumenstein, and S. Yu, "Detecting and mitigating poisoning attacks in federated learning using generative adversarial networks," *Concurrency Comput. Pract. Exper.*, vol. 34, no. 7, p. e5906, 2022.
- [31] S. Li, Y. Cheng, Y. Liu, W. Wang, and T. Chen, "Abnormal client behavior detection in federated learning," *arXiv preprint arXiv:1910.09933*, 2019.
- [32] Y. Jiang, W. Zhang, and Y. Chen, "Data quality detection mechanism against label flipping attacks in federated learning," *IEEE Trans. Inf. Forensics Security*, vol. 18, pp. 1625–1637, 2023.
- [33] P. R. Ovi, A. Gangopadhyay, R. F. Erbacher, and C. Busart, "Confident federated learning to tackle label flipped data poisoning attacks," in *Artificial Intelligence and Machine Learning for Multi-Domain Operations Applications V*, vol. 12538, 2023, pp. 263–272.
- [34] Y.-C. Lai, J.-Y. Lin, Y.-D. Lin, R.-H. Hwang, P.-C. Lin, H.-K. Wu, and C.-K. Chen, "Two-phase defense against poisoning attacks on federated learning-based intrusion detection," *Comput. Secur.*, vol. 129, p. 103205, 2023.
- [35] M. Mirza and S. Osindero, "Conditional generative adversarial nets," *arXiv preprint arXiv:1411.1784*, 2014.
- [36] W. Luo, "Efficient removal of impulse noise from digital images," *IEEE Trans. Consum. Electron.*, vol. 52, no. 2, pp. 523–527, 2006.

- [37] H. Note and Y. Denote, “On the proof of the law of the unconscious statistician,” 2018.
- [38] X. Chen, Y. Duan, R. Houthoof, J. Schulman, I. Sutskever, and P. Abbeel, “Infogan: Interpretable representation learning by information maximizing generative adversarial nets,” *NeurIPS*, vol. 29, 2016.
- [39] Y. LeCun, “The mnist database of handwritten digits,” <http://yann.lecun.com/exdb/mnist/>, 1998.
- [40] H. Xiao, K. Rasul, and R. Vollgraf, “Fashion-mnist: a novel image dataset for benchmarking machine learning algorithms,” *arXiv preprint arXiv:1708.07747*, 2017.
- [41] A. Krizhevsky, G. Hinton *et al.*, “Learning multiple layers of features from tiny images.(2009),” 2009.
- [42] O. Marfoq, G. Neglia, A. Bellet, L. Kameni, and R. Vidal, “Federated multi-task learning under a mixture of distributions,” *Adv. Neural Inf. Process. Syst.*, vol. 34, pp. 15 434–15 447, 2021.
- [43] X. Chen, C. Liu, B. Li, K. Lu, and D. Song, “Targeted backdoor attacks on deep learning systems using data poisoning,” *arXiv preprint arXiv:1712.05526*, 2017.